NASA
Technical Memorandum 4224

AVSCOM
Technical Report 90-B-007

Wind-Tunnel Survey of an Oscillating Flow Field for Application to Model Helicopter Rotor Testing

Paul H. Mirick, M-Nabil H. Hamouda,
and William T. Yeager, Jr.

DECEMBER 1990

NASA

US ARMY
AVIATION
SYSTEMS COMMAND
AVIATION R&T ACTIVITY

NASA
Technical Memorandum 4224

AVSCOM
Technical Report 90-B-007

Wind-Tunnel Survey of an Oscillating Flow Field for Application to Model Helicopter Rotor Testing

Paul H. Mirick
Aerostructures Directorate
USAARTA-AVSCOM
Langley Research Center
Hampton, Virginia

M-Nabil H. Hamouda
Lockheed Engineering & Sciences Company
Hampton, Virginia

William T. Yeager, Jr.
Aerostructures Directorate
USAARTA-AVSCOM
Langley Research Center
Hampton, Virginia

NASA
National Aeronautics and
Space Administration
Office of Management
Scientific and Technical
Information Division
1990

Summary

A survey of the flow field produced by the airstream oscillator system (AOS) in the Langley Transonic Dynamics Tunnel (TDT) is described in this report. The magnitude of the vertical and lateral gusts produced by the AOS was measured at 15 locations. The locations were selected to be in the plane of a typical model helicopter rotor when tested in the TDT using the aeroelastic rotor experimental system (ARES) model. These measurements were made over a range of tunnel dynamic pressures typical of those used for an ARES test. The data indicate that the gust field produced by the AOS is nonuniform across the tunnel test section, but that it should be sufficient to excite a model rotor.

Introduction

The gust response of helicopters has been the subject of study for some time. Helicopter gust response is important because of the conditions in which these aircraft operate. The helicopter must operate close to the ground (nap of the Earth), where the atmosphere may be turbulent, and make landings and takeoffs from small areas where winds in the proximity of trees and buildings can generate shear flows. In general, helicopters are less sensitive to gust-induced air loads than most fixed-wing aircraft. However, the blades of a rotor are much more responsive to gust loads than the aircraft as a whole. Also, if the helicopter is fitted with wings (e.g., compound configurations), additional gust loads may be generated. The successful application of advanced hub designs, such as hingeless and bearingless rotors, which may be more sensitive to gusts than articulated rotors because of larger hub moments, higher dynamic stress, and higher vibration levels, will require more research on rotor gust response for both handling qualities and loads.

The gust response of helicopter rotors has been the subject of several analytical studies, ranging from simplified analyses (refs. 1 to 3) to more sophisticated analytical models (ref. 4). Wind-tunnel tests are needed that provide data to validate these analytical efforts. These wind-tunnel tests should be conducted to evaluate the effects of a known gust field on blade response and on rotor loads and transient performance.

An initial effort to provide data that pertain to the effects of gusts that are appropriate to model helicopter rotors was conducted in the Langley Transonic Dynamics Tunnel (TDT). This initial effort consisted of a calibration of the oscillating gust field that was produced by the airstream oscillator system (AOS) of the TDT at dynamic pressures and at tunnel locations used for typical model rotor tests conducted on the aeroelastic rotor experimental system (ARES). The ARES model is the primary test-bed for rotorcraft tests conducted in the TDT. Measurements of the TDT oscillating gust field for fixed-wing-aircraft testing have been taken (refs. 5 to 7); however, for the effort described herein, the measurements are for lower dynamic pressures and were taken at more forward test-section locations than in the previous efforts.

Symbols

f	vane frequency of airstream oscillator system, Hz
q	free-stream dynamic pressure, lb/ft^2
V	free-stream velocity, ft/sec
x	tunnel station line, ft
y	tunnel spanwise station measured from centerline, ft
α	vertical flow angle, deg
β	lateral flow angle, deg
ω	circular frequency, $2\pi f$, rad/sec

Subscripts:

$1/2p\text{-}p$	one-half peak-to-peak value
norm	normalized

Apparatus and Procedures

The testing was conducted in the Langley Transonic Dynamics Tunnel (TDT). A schematic of the tunnel is shown in figure 1. The TDT is a continuous-flow tunnel with a slotted test section and is capable of operation up to Mach 1.2 at stagnation pressures up to 1 atm. The tunnel test section is 16 ft square with cropped corners and has a cross-sectional area of 248 ft^2. Either air or a heavy gas (R-12) may be used as a test medium. Because of its high density and low speed of sound relative to air, the use of R-12 aids the matching of model-rotor-scale Reynolds number and Mach number to full-scale values. The use of R-12 as a test medium also allows the easing of some restrictions on model structural design while still maintaining dynamic similarity. For example, the heavy-gas test medium permits a simplified structural design to obtain the required stiffness characteristics; therefore, the design and fabrication requirements of the model (ref. 8) are eased. For this investigation, R-12 at a nominal density of 0.006 slug/ft^3 was used as the test medium, because these conditions are representative of the majority of model rotor tests conducted in the TDT.

Airstream Oscillator System

The TDT is equipped with an airstream oscillator system (AOS), which uses short oscillating vanes that protrude from the tunnel walls to produce a sinusoidal disturbance in the tunnel flow. Figure 2 is a sketch of the AOS. The gust field is produced by induced flow associated with the trailing vortices from each vane tip. The vortices alternate in rotation direction as the vanes oscillate from positive to negative angles of attack, and the vortex system moves downstream with a wavelength, dependent upon frequency and free-stream velocity (ref. 5). The two sets of two vanes that comprise the AOS are mounted in a biplane configuration located at the entrance to the tunnel test section. Each vane is a semispan wing that utilizes a symmetrical airfoil section. The vanes have a span of 3.5 ft, a taper ratio of 0.5 (tip chord to root chord), and an aspect ratio of 1.2. Each set of biplane vanes is attached to a large flywheel. The vanes are oscillated about the quarter-chord by means of linkages connected to a flywheel that is driven by a hydraulic motor. This arrangement produces nearly sinusoidal oscillations about a preset vane angle of attack. The amplitude is mechanically adjustable from 0° to ±12°. For this test, the amplitude was set at 5.93° about a preset mean of 0°. The frequency of oscillation is remotely adjustable from 0 to 18 Hz by means of an electrical control system, which also synchronizes the motion of the two sets of vanes. The two vane sets can be operated either in phase or up to 180° out of phase. All data for this investigation were obtained with the vanes operating in phase.

Survey Device

The flow angularity of the airstream was measured with the survey device shown in figure 3. The survey device consisted of three flow-angularity-measurement assemblies mounted on two horizontal members that spanned the tunnel test section. The flow-angularity-measurement assemblies could be moved on the horizontal members of the survey device to any tunnel test-section span location desired. These three assemblies each used two balsa wood vanes, one to measure lateral β flow directions and the other to measure vertical α flow directions. The balsa vanes were rectangular, flat-plate configurations with aspect ratios of 0.5. Each vane was bonded to a stainless-steel leading edge and shaft adapter (fig. 4). An extension from the leading edge, located inboard of each balsa vane, provides the mass balance for each vane assembly. The vane assembly is pinned to a steel shaft, which is free to rotate in a hollow strut that projects from the housing. The outboard end of the shaft fits in a bronze sleeve bearing, and the inboard end of the shaft is attached to a low-torque potentiometer. The potentiometer is calibrated to provide the vane angular position. The survey device could also be moved fore and aft in the test section to cover a wide range of streamwise measurement locations. For this investigation, measurements were made within a 10-ft square (fig. 5) and 8 ft above the tunnel floor. These dimensions were chosen to cover the disk area of a rotor, up to 10 ft in diameter, being tested on the aeroelastic rotor experimental system (ARES) model (ref. 9). The ARES model is the test-bed most utilized for model rotor testing in the TDT.

Test Procedure

The purpose of this test was to determine the magnitude of the simulated gust field that could be produced in the plane of a typical model helicopter rotor being tested in the TDT with the ARES model. Gust-induced flow angles (or simply flow angles) were measured over a range of dynamic pressures from 10 to 50 psf. This range corresponds to a nominal range of model advance ratios from 0.17 to 0.40, where advance ratio is defined as the ratio of tunnel velocity to rotor rotational velocity. The range of advance ratios falls within the range for most model rotor tests conducted in the TDT. Initially, at each value of dynamic pressure, the AOS was operated at frequencies from 1 to 18 Hz. At AOS frequencies above 10 Hz, tunnel resonance effects became apparent. Similar observations were made in reference 5. Therefore, data presented in this report are limited to AOS frequencies of 10 Hz and below. At each combination of dynamic pressure and AOS frequency, flow-direction data were obtained from each flow-angularity-measurement assembly. These data were obtained by using the MODCOMP Classic 32 computer at a rate of 1000 data samples per second for 2.0 sec. The technique used to obtain the one-half peak-to-peak value of the flow angle was to first determine the arithmetic mean for 2000 data samples. The root-mean-square (RMS) of the deviation of each data sample from the arithmetic mean was then calculated and the one-half peak-to-peak value of the flow angle was determined by multiplying the RMS value by the square root of 2.

Presentation of Results

During this investigation, flow-angularity measurements were obtained at 15 locations in the tunnel test section at 5 values of tunnel dynamic pressure and a minimum of 6 values of AOS frequency. Because of the way the vertical and lateral vanes were mounted on the measurement assembly, the lateral measurement was always offset 8 in., both laterally and vertically from the vertical measurement. All data obtained in this test are contained in the appendix. However, for the purpose of this report, data are plotted at each test-section spanwise location at the three streamwise locations but for only three values of tunnel dynamic pressure and AOS frequency. This approach was taken because the plotted data are representative of the entire data set. The data consist of the one-half peak-to-peak value of the vertical- and lateral-flow angles as a function of test-section location. Data are also plotted in nondimensional form as normalized flow angle versus the wavelength parameter. The one-half peak-to-peak flow angle was normalized by the AOS maximum vane angle of attack, which for this test was 5.93°. The wavelength parameter is defined as the ratio of the AOS frequency to the tunnel free-stream velocity.

The data are presented in the following order:

	Figure
Spanwise variation of vertical-flow angle at tunnel station 62	6
Spanwise variation of lateral-flow angle at tunnel station 62	7
Longitudinal variation of vertical-flow angle at tunnel centerline	8
Longitudinal variation of lateral-flow angle 8 in. from tunnel centerline	9
Variation of normalized vertical-flow angle with wave parameter at tunnel centerline and station 62	10
Variation of normalized lateral-flow angle with wave parameter at tunnel centerline and station 62	11

Discussion of Results

Figure 6 shows the variation of the vertical-flow angle across the test section at tunnel station 62 as a function of the free-stream dynamic pressure q and AOS oscillation frequency. The cause of the nonuniform variation in flow angle across the test section is not known at this time. Similar spanwise variations of the vertical-flow field were obtained in a previous calibration effort (ref. 7). The data show that the vertical-flow angle generally increases by reducing the oscillation frequency of the AOS. Limited data obtained with the AOS stationary at 0° pitch angle (not presented here but included in the appendix) indicate that the flow angles produced by the tunnel turbulence level with the stationary AOS may not be any greater than that produced at higher AOS oscillation frequencies (above 5 Hz). Figure 7 shows the corresponding variation of the lateral-flow component across the tunnel test section. At the lowest value of dynamic pressure shown ($q =$ 10 lb/ft^2), the lateral-flow-angle amplitude shows a spanwise trend that is opposite that of the vertical-flow amplitude. This effect is not as significant at higher values of dynamic pressure. As dynamic pressure increases, the lateral-flow-angle amplitude is reduced and generally becomes more uniform across the test section.

Figures 8 and 9 show the streamwise variation of the vertical- and lateral-flow angles along the tunnel centerline. (The lateral-flow angles are measured 8 in. off the centerline.) These data are also typical of the flow angles measured on either side of the tunnel centerline and show no significant changes in the measured gust field as the measurement location in the test section is varied upstream and downstream.

Figures 10 and 11 present typical characteristics of the normalized vertical- and lateral-flow component measured during this investigation. The data of figure 10 are similar to results presented in reference 10. Based on the results of reference 10, the gust that is produced by the AOS should be sufficient for excitation of a model rotor over the range of conditions shown. The data show that the vertical-flow angle decreases as the value of the wave parameter increases, but the lateral-flow component is more constant. The wave parameter increases as wavelength decreases; therefore, the reduction in vertical-flow amplitude is most likely due to interaction and cancelling between vortices generated by the oscillating vanes. If the excitation of a particular model frequency is of interest for a given test, the test program should be planned such that the frequency of interest falls within the range of usable excitation shown in figure 10.

Conclusions

An investigation has been conducted in the Langley Transonic Dynamics Tunnel to measure the magnitude of the gust field that could be produced for use in the testing of model helicopter rotors. Based on the data obtained for the test conditions investigated, the following conclusions have been reached:

1. The gust field is nonuniform across the tunnel test section. The cause of this nonuniformity is not known at this time.

2. The magnitude of the gust field that is produced is sufficient to excite a model rotor.

Appendix

Presented in a tabular format in this appendix are one-half peak-to-peak values of the data obtained during the survey of the flow field produced by the airstream oscillator system (AOS) in the Langley Transonic Dynamics Tunnel.

There were six data runs made in the survey. In each run, the free-stream dynamic pressure q was varied from 10 to 50 lb/ft^2 in increments of 10 lb/ft^2. At each value of q, the AOS was varied from 0 to 10 Hz. From these data runs, flow-angularity measurements were obtained at 15 vane locations. In table A1, the positions of the alpha and betavanes are specified for the six data runs, and the corresponding data tables are identified.

Parts (a) and (b) of tables A2 to A7 present the data for the alpha vanes and the beta vanes, respectively. Presented in each table are the free-stream dynamic pressure q, the AOS frequency, the measured one-half peak-to-peak value of the vane angle, the calculated wave parameter (ratio of AOS frequency to tunnel free-stream velocity), and the normalized gust angle (measured one-half peak-to-peak value of the vane angle normalized by the preset maximum AOS angle). There was a problem with alpha vane 3, which caused some readings to be erroneous; these points are marked with an asterisk "*."

Table A1. Flow-Angularity-Measurement Positions

[Looking downstream, west is negative and east is positive; alpha vanes are 8 ft above tunnel floor; beta vanes are 7.333 ft above tunnel floor; see fig. 5 for clarification]

Data table	Tunnel station line	Alpha vane position, ft, for—			Beta vane position, ft, for—		
		Vane 1	Vane 2	Vane 3	Vane 1	Vane 2	Vane 3
A2(a)	57	−5.000	−2.500	0			
A2(b)	↓				−5.666	−3.166	−0.666
A3(a)	↓	0	2.500	5.000			
A3(b)	↓				−.666	1.833	4.333
A4(a)	62	−5.000	−2.500	0			
A4(b)	↓				−5.666	−3.166	−.666
A5(a)	↓	0	2.500	5.000			
A5(b)	↓				−.666	1.833	4.333
A6(a)	67	−5.000	−2.500	0			
A6(b)	↓				−5.666	−3.166	−.666
A7(a)	↓	0	2.500	5.000			
A7(b)	↓				−.666	1.833	4.333

Table A2. Flow-Angularity Measurement for Station 57 West

(a) Alpha (vertical) calibration rig position

[There was a problem with alpha vane 3, which caused some readings to be erroneous; these points are marked with an asterisk "*"]

q, lb/ft^2	AOS frequency, Hz	1/2p-p flow angle, deg, for—			Wave parameter	Normalized flow angle, deg, for—		
		Vane 1	Vane 2	Vane 3		Vane 1	Vane 2	Vane 3
10	0	0.215	0.439	0.031	0.000	0.036	0.074	0.005
10	1	.255	1.143	.584	.110	.043	.193	.098
10	2	.218	.504	.240	.221	.037	.085	.040
10	3	.231	.429	.050	.331	.039	.072	.008
10	4	.104	.188	.130	.442	.018	.032	.022
10	4	.233	.175	.094	.442	.039	.030	.016
10	5	.210	.145	.052	.552	.035	.024	.009
10	10	.014	.185	.032	1.110	.002	.031	.005
20	0	.256	.257	.274	.000	.043	.043	.046
20	0	.293	.246	.323	.000	.049	.041	.054
20	1	.584	1.143	.931	.078	.098	.193	.157
20	1	.531	1.000	.945	.077	.090	.169	.159
20	2	.401	.630	.573	.156	.068	.106	.097
20	2	.455	.852	.659	.157	.077	.144	.111
20	3	.405	.471	.396	.235	.068	.079	.067
20	3	.379	.383	.384	.234	.064	.065	.065
20	4	.459	.373	.306	.314	.077	.063	.052
20	4	.380	.250	.322	.311	.064	.042	.054
20	5	.420	.294	.292	.390	.071	.050	.049
20	5	.364	.250	.273	.390	.061	.042	.046
20	10	.330	.251	.310	.782	.056	.042	.052
20	10	.286	.278	*	.782	.048	.047	*
30	0	.250	.596	.247	.000	.042	.101	.042
30	1	.583	1.236	.796	.064	.098	.208	.134
30	2	.404	1.197	*	.127	.068	.202	*
30	3	.369	.741	.378	.191	.062	.125	.064
30	4	.367	.807	.315	.255	.062	.136	.053
30	5	.366	.870	.255	.318	.062	.147	.043
30	10	.269	1.896	.295	.637	.045	.320	.050
40	0	.259	.953	.244	.000	.044	.161	.041
40	1	.644	1.640	*	.055	.109	.277	*
40	1	.503	2.311	.782	.055	.085	.390	.132
40	2	.369	1.166	.666	.110	.062	.197	.112
40	2	.382	2.400	.660	.110	.064	.405	.111
40	3	.269	.922	.547	.165	.045	.155	.092
40	4	.319	.848	.364	.220	.054	.143	.061
40	4	.333	.698	*	.220	.056	.118	*
40	4	.326	1.604	.411	.220	.055	.270	.069
40	5	.328	1.268	.370	.275	.055	.214	.062
40	5	.333	.656	.288	.275	.056	.111	.049
40	10	.288	.813	.247	.551	.049	.137	.042
40	10	.284	.718	.265	.551	.048	.121	.045
50	0	.184	1.127	.230	.000	.031	.190	.039
50	1	.627	1.889	1.018	.049	.106	.319	.172
50	2	.541	1.233	.803	.098	.091	.208	.135
50	3	.343	.875	.433	.148	.058	.148	.073
50	4	.307	.809	.416	.196	.052	.136	.070
50	5	.349	1.028	.242	.245	.059	.173	.041
50	10	.419	.896	.236	.491	.071	.151	.040

Table A2. Concluded

(b) Beta (lateral) calibration rig position

q, lb/ft^2	AOS frequency, Hz	1/2*p-p* flow angle, deg, for—			Wave parameter	Normalized flow angle, deg, for—		
		Vane 1	Vane 2	Vane 3		Vane 1	Vane 2	Vane 3
10	0	0.706	0.111	0.259	0.000	0.119	0.019	0.044
10	1	1.312	.267	.298	.110	.221	.045	.050
10	2	1.206	.164	.318	.221	.203	.028	.054
10	3	1.874	.148	.224	.331	.316	.025	.038
10	4	1.039	.186	.258	.442	.175	.031	.044
10	4	1.097	.141	.215	.442	.185	.024	.036
10	5	.944	.175	.253	.552	.159	.030	.043
10	10	.412	.145	.207	1.110	.069	.024	.035
20	0	1.132	.231	.252	.000	.191	.039	.043
20	0	2.282	.158	.268	.000	.385	.027	.045
20	1	1.838	.189	.280	.078	.310	.032	.047
20	1	1.452	.214	.341	.077	.245	.036	.057
20	2	1.284	.198	.269	.156	.217	.033	.045
20	2	1.713	.160	.219	.157	.289	.027	.037
20	3	1.444	.161	.283	.235	.244	.027	.048
20	3	1.132	.198	.257	.234	.191	.033	.043
20	4	.997	.222	.290	.314	.168	.037	.049
20	4	.927	.169	.269	.311	.156	.028	.045
20	5	.857	.197	.260	.390	.145	.033	.044
20	5	.705	.184	.266	.390	.119	.031	.045
20	10	.449	.154	.252	.782	.076	.026	.043
20	10	.438	.156	.261	.782	.074	.026	.044
30	0	1.728	.190	.262	.000	.291	.032	.044
30	1	1.578	.180	.258	.064	.266	.030	.043
30	2	1.657	.200	.255	.127	.279	.034	.043
30	3	1.271	.154	.238	.191	.214	.026	.040
30	4	.989	.187	.209	.255	.167	.032	.035
30	5	.888	.184	.223	.318	.150	.031	.038
30	10	.488	.193	.189	.637	.082	.032	.032
40	0	1.963	.111	.259	.000	.331	.019	.044
40	1	1.895	.158	.273	.055	.320	.027	.046
40	1	1.493	.145	.221	.055	.252	.025	.037
40	2	1.388	.139	.203	.110	.234	.023	.034
40	2	1.589	.144	.249	.110	.268	.024	.042
40	3	1.182	.160	.258	.165	.199	.027	.043
40	4	1.049	.175	.197	.220	.177	.029	.033
40	4	.957	.241	.240	.220	.161	.041	.040
40	4	.910	.433	.247	.220	.153	.073	.042
40	5	.756	.216	.261	.275	.127	.036	.044
40	5	.780	.213	.255	.275	.131	.036	.043
40	10	.420	.181	.222	.551	.071	.031	.038
40	10	.435	.190	.256	.551	.073	.032	.043
50	0	2.534	.139	.286	.000	.427	.023	.048
50	1	1.656	.222	.234	.049	.279	.037	.040
50	2	1.638	.170	.259	.098	.276	.029	.044
50	3	1.450	.169	.263	.148	.244	.029	.044
50	4	1.089	.201	.251	.196	.184	.034	.042
50	5	.793	.200	.280	.245	.134	.034	.047
50	10	.529	.198	.254	.491	.089	.033	.043

Table A3. Flow-Angularity Measurement for Station 57 East

(a) Alpha (vertical) calibration rig position

q, lb/ft^2	AOS frequency, Hz	1/2p-p flow angle, deg, for—			Wave parameter	Normalized flow angle, deg, for—		
		Vane 1	Vane 2	Vane 3		Vane 1	Vane 2	Vane 3
10	0	0.255	0.349	0.226	0.000	0.043	0.059	0.038
10	1	.745	.897	.332	.109	.126	.151	.056
10	1	.649	.839	.381	.109	.109	.141	.064
10	2	.302	.481	.358	.219	.051	.081	.060
10	2	.271	.556	.366	.220	.046	.094	.062
10	3	.246	.513	.264	.328	.041	.087	.045
10	3	.294	.341	.289	.330	.050	.058	.049
10	4	.211	.356	.294	.442	.036	.060	.050
10	4	.138	.372	.308	.440	.023	.063	.052
10	5	.233	.337	.330	.550	.039	.057	.056
10	5	.195	.430	.317	.553	.033	.073	.053
10	10	.237	.400	.264	1.100	.040	.067	.045
10	10	.217	.323	.247	1.106	.037	.054	.042
20	0	.244	.298	.175	.000	.041	.050	.030
20	0	.332	.415	.215	.000	.056	.070	.036
20	1	.919	.960	.373	.078	.155	.162	.063
20	1	.999	1.027	.405	.078	.168	.173	.068
20	1	.971	1.000	.403	.078	.164	.169	.068
20	1	1.000	1.207	.326	.077	.169	.204	.055
20	2	.605	.579	.366	.155	.102	.098	.062
20	2	.647	.694	.269	.155	.109	.117	.045
20	2	.580	.621	.327	.156	.098	.105	.055
20	2	.510	.719	.295	.155	.086	.121	.050
20	3	.362	.727	.359	.233	.061	.123	.061
20	3	.319	.628	.322	.233	.054	.106	.054
20	3	.386	.574	.267	.233	.065	.097	.045
20	3	.312	.505	.390	.234	.053	.085	.066
20	4	.598	1.016	.304	.310	.101	.171	.051
20	4	.289	.647	.322	.311	.049	.109	.054
20	4	.271	.545	.296	.310	.046	.092	.050
20	4	.328	.783	.347	.311	.055	.132	.059
20	5	.357	.790	.264	.388	.060	.133	.045
20	5	.266	.761	.308	.387	.045	.128	.052
20	5	.353	.861	.294	.387	.060	.145	.050
20	5	.292	.656	.322	.388	.049	.111	.054
20	10	.264	.770	.226	.777	.045	.130	.038
20	10	.277	.835	.205	.779	.047	.141	.035
20	10	.399	.759	.296	.779	.067	.128	.050
20	10	.368	.862	.237	.777	.062	.145	.040
30	0	.212	.911	.211	.000	.036	.154	.036
30	0	.240	.902	.215	.000	.040	.152	.036
30	1	1.019	1.248	.332	.064	.172	.210	.056
30	1	1.010	1.210	.307	.064	.170	.204	.052
30	2	.704	.956	.204	.128	.119	.161	.034
30	2	.692	.914	.180	.128	.117	.154	.030
30	3	.335	.791	.275	.191	.056	.133	.046
30	3	.405	.858	.171	.191	.068	.145	.029
30	4	.333	.955	.293	.255	.056	.161	.049
30	4	.287	.947	.212	.256	.048	.160	.036

Table A3. Continued

(a) Concluded

[There was a problem with alpha vane 3, which caused some readings to be erroneous; these points are marked with an asterisk "*"]

q, lb/ft^2	AOS frequency, Hz	1/2p-p flow angle, deg, for— Vane 1	Vane 2	Vane 3	Wave parameter	Normalized flow angle, deg, for— Vane 1	Vane 2	Vane 3
30	5	0.287	0.916	0.216	0.320	0.048	0.154	0.036
30	5	.195	.906	.268	.319	.033	.153	.045
30	10	.222	.589	.248	.640	.037	.099	.042
30	10	.246	.611	.248	.640	.041	.103	.042
40	0	.259	.638	.135	.000	.044	.108	.023
40	0	.255	.975	.124	.000	.043	.164	.021
40	0	.278	.592	.233	.000	.047	.100	.039
40	0	.249	.468	*	.000	.042	.079	*
40	1	.985	1.243	.284	.055	.166	.210	.048
40	1	1.070	1.360	.304	.055	.180	.229	.051
40	1	.925	1.230	.300	.055	.156	.207	.051
40	1	1.055	1.239	.266	.055	.178	.209	.045
40	2	.764	.906	.213	.110	.129	.153	.036
40	2	.751	.858	.189	.110	.127	.145	.032
40	2	.725	.921	.153	.110	.122	.155	.026
40	2	.651	.996	.176	.110	.110	.168	.030
40	3	.498	.669	.211	.165	.084	.113	.036
40	3	.602	.656	.205	.165	.102	.111	.035
40	3	.501	.611	.188	.165	.084	.103	.032
40	3	.549	.647	.134	.165	.093	.109	.023
40	4	.355	.584	.189	.220	.060	.098	.032
40	4	.400	.511	.189	.220	.067	.086	.032
40	4	.411	.482	.179	.220	.069	.081	.030
40	4	.369	.481	.186	.220	.062	.081	.031
40	5	.309	.546	.215	.275	.052	.092	.036
40	5	.412	.570	.178	.275	.069	.096	.030
40	5	.260	.518	.195	.275	.044	.087	.033
40	5	.281	.578	.198	.276	.047	.097	.033
40	10	.333	.505	*	.552	.056	.085	*
40	10	.262	.472	.078	.552	.044	.080	.013
40	10	.300	.626	.148	.552	.051	.106	.025
40	10	.309	.664	.111	.551	.052	.112	.019
50	0	.235	.649	.200	.000	.040	.109	.034
50	0	.287	.638	*	.000	.048	.108	*
50	1	.979	1.208	.355	.049	.165	.204	.060
50	1	1.047	1.338	.368	.049	.177	.226	.062
50	2	.899	.982	.210	.098	.152	.166	.035
50	2	.846	.931	.193	.098	.143	.157	.033
50	3	.674	.750	.183	.147	.114	.126	.031
50	3	.595	.739	.109	.147	.100	.125	.018
50	4	.463	.646	.146	.196	.078	.109	.025
50	4	.409	.671	.166	.196	.069	.113	.028
50	5	.341	.765	.200	.245	.058	.129	.034
50	5	.368	.736	.195	.246	.062	.124	.033
50	10	.250	.780	.125	.491	.042	.132	.021
50	10	.238	.877	.072	.492	.040	.148	.012

Table A3. Continued

(b) Beta (lateral) calibration rig position

q, lb/ft^2	AOS frequency, Hz	1/2*p-p* flow angle, deg, for—			Wave parameter	Normalized flow angle, deg, for—		
		Vane 1	Vane 2	Vane 3		Vane 1	Vane 2	Vane 3
10	0	0.495	0.016	0.253	0.000	0.084	0.003	0.043
10	1	.624	.133	.621	.109	.105	.022	.105
10	1	.438	.044	.599	.109	.074	.007	.101
10	2	.472	.084	.387	.219	.080	.014	.065
10	2	.644	.135	.442	.220	.109	.023	.074
10	3	.614	.172	.310	.328	.104	.029	.052
10	3	.715	.171	.361	.330	.121	.029	.061
10	4	.658	.191	.312	.442	.111	.032	.053
10	4	.920	.160	.304	.440	.155	.027	.051
10	5	.550	.206	.318	.550	.093	.035	.054
10	5	.601	.196	.243	.553	.101	.033	.041
10	10	.582	.204	.211	1.100	.098	.034	.036
10	10	.632	.200	.174	1.106	.107	.034	.029
20	0	.267	.179	.236	.000	.045	.030	.040
20	0	.255	.095	.267	.000	.043	.016	.045
20	1	.271	.171	.512	.078	.046	.029	.086
20	1	.257	.191	.539	.078	.043	.032	.091
20	1	.283	.193	.607	.078	.048	.033	.102
20	1	.259	.178	.511	.077	.044	.030	.086
20	2	.279	.170	.445	.155	.047	.029	.075
20	2	.251	.243	.379	.155	.042	.041	.064
20	2	.262	.135	.394	.156	.044	.023	.066
20	2	.271	.208	.425	.155	.046	.035	.072
20	3	.258	.189	.378	.233	.043	.032	.064
20	3	.217	.326	.349	.233	.037	.055	.059
20	3	.273	.131	.343	.233	.046	.022	.058
20	3	.289	.156	.336	.234	.049	.026	.057
20	4	.245	.168	.317	.310	.041	.028	.053
20	4	.263	.228	.376	.311	.044	.039	.063
20	4	.255	.201	.316	.310	.043	.034	.053
20	4	.268	.199	.261	.311	.045	.033	.044
20	5	.269	.156	.300	.388	.045	.026	.051
20	5	.235	.162	.317	.387	.040	.027	.053
20	5	.246	.188	.298	.387	.041	.032	.050
20	5	.255	.154	.295	.388	.043	.026	.050
20	10	.159	.301	.301	.777	.027	.051	.051
20	10	.200	.188	.252	.779	.034	.032	.042
20	10	.238	.292	.256	.779	.040	.049	.043
20	10	.221	.440	.277	.777	.037	.074	.047
30	0	.249	.783	.283	.000	.042	.132	.048
30	0	.253	.132	.271	.000	.043	.022	.046
30	1	.245	.412	.559	.064	.041	.069	.094
30	1	.236	.715	.553	.064	.040	.121	.093
30	2	.259	.438	.470	.128	.044	.074	.079
30	2	.241	.877	.460	.128	.041	.148	.078
30	3	.288	.176	.405	.191	.049	.030	.068
30	3	.248	.526	.390	.191	.042	.089	.066
30	4	.274	.154	.392	.255	.046	.026	.066
30	4	.256	.090	.391	.256	.043	.015	.066

Table A3. Concluded

(b) Concluded

q, lb/ft^2	AOS frequency, Hz	1/2*p-p* flow angle, deg, for— Vane 1	Vane 2	Vane 3	Wave parameter	Normalized flow angle, deg, for— Vane 1	Vane 2	Vane 3
30	5	0.231	0.140	0.342	0.320	0.039	0.024	0.058
30	5	.267	.154	.393	.319	.045	.026	.066
30	10	.223	.148	.268	.640	.038	.025	.045
30	10	.221	.164	.270	.640	.037	.028	.046
40	0	.291	.120	.252	.000	.049	.020	.042
40	0	.221	.182	.261	.000	.037	.031	.044
40	0	.258	.119	.266	.000	.044	.020	.045
40	0	.203	.163	.259	.000	.034	.027	.044
40	1	.258	.340	.601	.055	.044	.057	.101
40	1	.209	.102	.622	.055	.035	.017	.105
40	1	.184	.157	.606	.055	.031	.026	.102
40	1	.221	.541	.665	.055	.037	.091	.112
40	2	.195	.117	.584	.110	.033	.020	.098
40	2	.277	.133	.563	.110	.047	.022	.095
40	2	.186	.226	.530	.110	.031	.038	.089
40	2	.218	.142	.504	.110	.037	.024	.085
40	3	.242	.123	.478	.165	.041	.021	.081
40	3	.197	.128	.367	.165	.033	.022	.062
40	3	.236	.153	.399	.165	.040	.026	.067
40	3	.239	.159	.469	.165	.040	.027	.079
40	4	.252	.140	.374	.220	.042	.024	.063
40	4	.220	.147	.371	.220	.037	.025	.063
40	4	.244	.139	.358	.220	.041	.023	.060
40	4	.263	.152	.402	.220	.044	.026	.068
40	5	.220	.151	.347	.275	.037	.026	.059
40	5	.204	.163	.338	.275	.034	.028	.057
40	5	.190	.160	.317	.275	.032	.027	.053
40	5	.229	.156	.339	.276	.039	.026	.057
40	10	.246	.195	.373	.552	.041	.033	.063
40	10	.205	.183	.277	.552	.035	.031	.047
40	10	.226	.198	.321	.552	.038	.033	.054
40	10	.236	.187	.336	.551	.040	.032	.057
50	0	.206	.194	.298	.000	.035	.033	.050
50	0	.275	.204	.269	.000	.046	.034	.045
50	1	.294	.180	.502	.049	.050	.030	.085
50	1	.247	.188	.625	.049	.042	.032	.105
50	2	.253	.203	.522	.098	.043	.034	.088
50	2	.231	.165	.583	.098	.039	.028	.098
50	3	.228	.148	.512	.147	.038	.025	.086
50	3	.219	.183	.479	.147	.037	.031	.081
50	4	.245	.178	.402	.196	.041	.030	.068
50	4	.222	.160	.387	.196	.038	.027	.065
50	5	.248	.123	.347	.245	.042	.021	.058
50	5	.253	.124	.393	.246	.043	.021	.066
50	10	.243	.168	.283	.491	.041	.028	.048
50	10	.227	.163	.292	.492	.038	.028	.049

Table A4. Flow-Angularity Measurement for Station 62 West

(a) Alpha (vertical) calibration rig position

[There was a problem with alpha vane 3, which caused some readings to be erroneous; these points are marked with an asterisk "*"]

q, lb/ft^2	AOS frequency, Hz	1/2p-p flow angle, deg, for—			Wave parameter	Normalized flow angle, deg, for—		
		Vane 1	Vane 2	Vane 3		Vane 1	Vane 2	Vane 3
10	1	0.097	0.952	0.462	0.111	0.016	0.161	0.078
10	2	.224	.785	.240	.223	.038	.132	.040
10	3	.231	.878	.238	.336	.039	.148	.040
10	4	.174	1.051	.220	.445	.029	.177	.037
10	5	.045	1.026	.153	.554	.008	.173	.026
10	10	.225	1.231	.204	1.118	.038	.208	.034
20	1	.510	1.038	.718	.078	.086	.175	.121
20	1	.580	1.051	.703	.077	.098	.177	.119
20	2	.354	.695	.396	.155	.060	.117	.067
20	2	.370	.780	.477	.155	.062	.131	.080
20	3	.366	.531	.227	.233	.062	.090	.038
20	3	.320	.414	.253	.232	.054	.070	.043
20	4	.401	.298	.175	.310	.068	.050	.030
20	4	.339	.441	.209	.310	.057	.074	.035
20	5	.331	.411	.220	.388	.056	.069	.037
20	5	.375	.535	.219	.388	.063	.090	.037
20	10	.253	.423	.185	.778	.043	.071	.031
20	10	.223	.328	.219	.778	.038	.055	.037
30	1	.543	1.264	.808	.064	.092	.213	.136
30	2	.282	1.088	.456	.127	.048	.183	.077
30	3	.286	.823	.322	.191	.048	.139	.054
30	4	.365	.716	.261	.256	.062	.121	.044
30	5	.381	.681	.249	.319	.064	.115	.042
30	10	.237	.833	.283	.640	.040	.140	.048
40	1	.578	1.183	.754	.055	.097	.199	.127
40	1	.497	1.378	.811	.055	.084	.232	.137
40	2	.297	.941	.536	.110	.050	.159	.090
40	2	.297	1.113	.617	.110	.050	.188	.104
40	3	.292	.962	.357	.165	.049	.162	.060
40	3	.290	1.251	.336	.165	.049	.211	.057
40	4	.341	1.096	.305	.220	.058	.185	.051
40	4	.360	.775	.247	.220	.061	.131	.042
40	5	.312	.804	.302	.275	.053	.136	.051
40	5	.375	.887	.287	.275	.063	.150	.048
40	10	.310	.839	.291	.551	.052	.141	.049
40	10	.288	.836	.240	.551	.049	.141	.040
50	1	.588	1.360	.826	.049	.099	.229	.139
50	2	.334	1.404	.689	.098	.056	.237	.116
50	3	.333	.695	.399	.147	.056	.117	.067
50	4	.334	.661	.299	.196	.056	.111	.050
50	5	.411	.625	.263	.246	.069	.105	.044
50	10	.364	.503	*	.492	.061	.085	*

Table A4. Concluded

(b) Beta (lateral) calibration rig position

q, lb/ft^2	AOS frequency, Hz	1/2*p*-*p* flow angle, deg, for—			Wave parameter	Normalized flow angle, deg, for—		
		Vane 1	Vane 2	Vane 3		Vane 1	Vane 2	Vane 3
10	1	1.646	0.180	0.267	0.111	0.278	0.030	0.045
10	2	1.732	.141	.254	.223	.292	.024	.043
10	3	1.415	.146	.251	.336	.239	.025	.042
10	4	1.054	.167	.256	.445	.178	.028	.043
10	5	.836	.169	.260	.554	.141	.028	.044
10	10	.399	.138	.255	1.118	.067	.023	.043
20	1	1.869	.267	.234	.078	.315	.045	.039
20	1	1.777	.266	.222	.077	.300	.045	.037
20	2	1.966	.246	.283	.155	.332	.041	.048
20	2	1.700	.780	.294	.155	.287	.131	.050
20	3	1.465	.228	.245	.233	.247	.038	.041
20	3	1.450	.217	.269	.232	.244	.037	.045
20	4	1.322	.202	.254	.310	.223	.034	.043
20	4	1.195	.223	.314	.310	.201	.038	.053
20	5	1.003	.215	.283	.388	.169	.036	.048
20	5	1.094	.192	.279	.388	.184	.032	.047
20	10	.514	.186	.215	.778	.087	.031	.036
20	10	.382	.277	.266	.778	.064	.047	.045
30	1	1.458	.290	.240	.064	.246	.049	.041
30	2	1.711	.208	.275	.127	.289	.035	.046
30	3	1.397	.225	.208	.191	.236	.038	.035
30	4	1.091	.198	.274	.256	.184	.033	.046
30	5	1.081	.219	.288	.319	.182	.037	.049
30	10	.503	.187	.254	.640	.085	.032	.043
40	1	1.764	.181	.252	.055	.298	.031	.043
40	1	1.734	.245	.254	.055	.292	.041	.043
40	2	1.626	.195	.245	.110	.274	.033	.041
40	2	1.664	.237	.226	.110	.281	.040	.038
40	3	1.312	.174	.264	.165	.221	.029	.044
40	3	1.245	.329	.262	.165	.210	.056	.044
40	4	1.170	.223	.260	.220	.197	.038	.044
40	4	1.079	.197	.261	.220	.182	.033	.044
40	5	1.002	.263	.236	.275	.169	.044	.040
40	5	.950	.286	.305	.275	.160	.048	.051
40	10	.474	.148	.215	.551	.080	.025	.036
40	10	.495	.627	.191	.551	.084	.106	.032
50	1	1.686	.204	.241	.049	.284	.034	.041
50	2	1.495	.259	.232	.098	.252	.044	.039
50	3	1.529	.193	.277	.147	.258	.033	.047
50	4	1.124	.331	.289	.196	.189	.056	.049
50	5	.908	.694	.247	.246	.153	.117	.042
50	10	.509	.790	.228	.492	.086	.133	.038

Table A5. Flow-Angularity Measurement for Station 62 East

(a) Alpha (vertical) calibration rig position

[There was a problem with alpha vane 3, which caused some readings to be erroneous; these points are marked with an asterisk "*"]

q, lb/ft^2	AOS frequency, Hz	1/2p-p flow angle, deg, for— Vane 1	Vane 2	Vane 3	Wave parameter	Normalized flow angle, deg, for— Vane 1	Vane 2	Vane 3
10	0	0.227	0.587	0.239	0.000	0.038	0.099	0.040
10	0	.199	.791	.190	.000	.034	.133	.032
10	1	.709	.961	.248	.110	.120	.162	.042
10	1	.664	.963	.295	.110	.112	.162	.050
10	2	.252	.836	.301	.220	.042	.141	.051
10	2	.283	.765	*	.220	.048	.129	*
10	3	.248	.631	.273	.330	.042	.106	.046
10	3	.218	.484	.231	.330	.037	.082	.039
10	4	.241	.520	.296	.440	.041	.088	.050
10	4	.238	.572	.263	.438	.040	.096	.044
10	5	.252	.540	.249	.550	.042	.091	.042
10	5	.211	.580	.262	.547	.036	.098	.044
10	10	.092	.576	.164	1.105	.016	.097	.028
10	10	.238	.652	.048	1.105	.040	.110	.008
20	0	.295	.546	.261	.000	.050	.092	.044
20	0	.269	.562	.268	.000	.045	.095	.045
20	0	.234	.353	.272	.000	.039	.060	.046
20	0	.238	.450	.328	.000	.040	.076	.055
20	1	1.027	1.229	.370	.078	.173	.207	.062
20	1	.918	1.186	.296	.077	.155	.200	.050
20	1	.974	1.153	.305	.078	.164	.194	.051
20	1	.917	1.100	.352	.078	.155	.185	.059
20	2	.622	.809	.311	.157	.105	.136	.052
20	2	.487	.735	.293	.155	.082	.124	.049
20	2	.607	.679	.312	.156	.102	.115	.053
20	2	.634	.776	.267	.156	.107	.131	.045
20	3	.344	.459	.314	.234	.058	.077	.053
20	3	.384	.526	.316	.234	.065	.089	.053
20	3	.320	.484	.325	.235	.054	.082	.055
20	3	.283	.519	.332	.234	.048	.088	.056
20	4	.248	.392	.307	.313	.042	.066	.052
20	4	.262	.421	.369	.314	.044	.071	.062
20	4	.277	.492	.398	.312	.047	.083	.067
20	4	.266	.427	.329	.311	.045	.072	.055
20	5	.253	.456	.324	.391	.043	.077	.055
20	5	.310	.403	.344	.392	.052	.068	.058
20	5	.300	.480	.338	.391	.051	.081	.057
20	5	.276	.420	.293	.391	.047	.071	.049
20	10	.263	.393	.298	.781	.044	.066	.050
20	10	.248	.415	.249	.784	.042	.070	.042
20	10	.255	.463	.282	.786	.043	.078	.048
20	10	.282	.382	.275	.784	.048	.064	.046
30	0	.242	.191	.205	.000	.041	.032	.035
30	0	.245	.177	.177	.000	.041	.030	.030
30	1	1.026	1.226	.233	.064	.173	.207	.039
30	1	.959	1.151	.364	.064	.162	.194	.061
30	2	.587	.737	.306	.128	.099	.124	.052
30	2	.604	.792	.302	.127	.102	.134	.051
30	3	.388	.481	.258	.192	.065	.081	.044

Table A5. Continued

(a) Concluded

[There was a problem with alpha vane 3, which caused some readings to be erroneous; these points are marked with an asterisk "*"]

q, lb/ft^2	AOS frequency, Hz	1/2p-p flow angle, deg, for—			Wave parameter	Normalized flow angle, deg, for—		
		Vane 1	Vane 2	Vane 3		Vane 1	Vane 2	Vane 3
30	3	0.385	0.500	*	0.192	0.065	0.084	*
30	4	.332	.303	.285	.255	.056	.051	.048
30	4	.280	.313	.254	.256	.047	.053	.043
30	5	.248	.301	.213	.320	.042	.051	.036
30	5	.262	.272	.241	.320	.044	.046	.041
30	10	.252	.216	.221	.638	.042	.036	.037
30	10	.255	.203	*	.641	.043	.034	*
40	0	.245	.314	.209	.000	.041	.053	.035
40	0	.255	.549	.221	.000	.043	.093	.037
40	0	.162	.470	.111	.000	.027	.079	.019
40	0	.283	.379	.189	.000	.048	.064	.032
40	1	.949	1.296	*	.055	.160	.219	*
40	1	.920	1.231	.248	.055	.155	.208	.042
40	1	.956	1.246	.305	.055	.161	.210	.051
40	1	1.019	1.259	.269	.055	.172	.212	.045
40	2	.718	1.011	.241	.110	.121	.170	.041
40	2	.783	1.097	.225	.110	.132	.185	.038
40	2	.711	1.019	.192	.110	.120	.172	.032
40	2	.632	.981	.238	.110	.107	.165	.040
40	3	.412	.836	.256	.165	.069	.141	.043
40	3	.463	.735	.362	.165	.078	.124	.061
40	3	.492	.739	.232	.165	.083	.125	.039
40	3	.484	.815	.241	.165	.082	.137	.041
40	4	.294	.523	.311	.220	.050	.088	.052
40	4	.333	.577	.240	.220	.056	.097	.040
40	4	.289	.534	.231	.219	.049	.090	.039
40	4	.390	.535	.230	.220	.066	.090	.039
40	5	.265	.555	.396	.274	.045	.094	.067
40	5	.254	.427	.400	.275	.043	.072	.067
40	5	.252	.559	.359	.274	.042	.094	.061
40	5	.319	.495	.321	.274	.054	.083	.054
40	10	.221	.486	.427	.550	.037	.082	.072
40	10	.218	.444	.343	.550	.037	.075	.058
40	10	.217	.432	.333	.550	.037	.073	.056
40	10	.259	.458	.291	.550	.044	.077	.049
50	0	.287	.371	*	.000	.048	.063	*
50	0	.310	.458	.250	.000	.052	.077	.042
50	1	1.041	1.286	.276	.049	.176	.217	.047
50	1	.969	1.351	.239	.049	.163	.228	.040
50	2	.846	1.127	*	.098	.143	.190	*
50	2	.750	1.215	.208	.098	.126	.205	.035
50	3	.575	.969	.312	.148	.097	.163	.053
50	3	.634	.806	.310	.148	.107	.136	.052
50	4	.497	.766	.283	.197	.084	.129	.048
50	4	.467	.688	.419	.196	.079	.116	.071
50	5	.388	.586	.514	.245	.065	.099	.087
50	5	.408	.523	.387	.245	.069	.088	.065
50	10	.293	.466	.468	.491	.049	.079	.079
50	10	.344	.480	.444	.491	.058	.081	.075

Table A5. Continued

(b) Beta (lateral) calibration rig position

q, lb/ft^2	AOS frequency, Hz	1/2p-p flow angle, deg, for—			Wave parameter	Normalized flow angle, deg, for—		
		Vane 1	Vane 2	Vane 3		Vane 1	Vane 2	Vane 3
20	0	0.265	0.199	0.256	0.000	0.045	0.034	0.043
20	0	.283	.072	.269	.000	.0048	.012	.045
20	0	.254	.252	.233	.000	.043	.043	.039
20	0	.273	.171	.269	.000	.046	.029	.045
20	1	.273	.157	.571	.078	.046	.026	.096
20	1	.283	.179	.568	.077	.048	.030	.096
20	1	.285	.098	.624	.078	.048	.017	.105
20	1	.259	.175	.565	.078	.044	.029	.095
20	2	.265	.272	.367	.157	.045	.046	.062
20	2	.251	.185	.420	.155	.042	.031	.071
20	2	.276	.192	.361	.156	.047	.032	.061
20	2	.262	.247	.410	.156	.044	.042	.069
20	3	.292	.269	.316	.234	.049	.045	.053
20	3	.249	.191	.295	.234	.042	.032	.050
20	3	.278	.295	.336	.235	.047	.050	.057
20	3	.300	.203	.294	.234	.051	.034	.050
20	4	.237	.331	.327	.313	.040	.056	.055
20	4	.292	.214	.307	.314	.049	.036	.052
20	4	.258	.234	.291	.312	.043	.039	.049
20	4	.271	.212	.310	.311	.046	.036	.052
20	5	.236	.275	.313	.391	.040	.046	.053
20	5	.248	.223	.294	.392	.042	.038	.050
20	5	.260	.201	.304	.391	.044	.034	.051
20	5	.289	.285	.275	.391	.049	.048	.046
20	10	.250	.243	.200	.781	.042	.041	.034
20	10	.287	.226	.211	.784	.048	.038	.036
20	10	.259	.271	.311	.786	.044	.046	.052
20	10	.255	.247	.241	.784	.043	.042	.041
30	0	.289	.132	.289	.000	.049	.022	.049
30	0	.244	.242	.226	.000	.041	.041	.038
30	1	.292	.553	.602	.064	.049	.093	.101
30	1	.259	.537	.548	.064	.044	.091	.092
30	2	.209	.860	.474	.128	.035	.145	.080
30	2	.276	.219	.502	.127	.047	.037	.085
30	3	.264	.330	.419	.192	.044	.056	.071
30	3	.236	.482	.342	.192	.040	.081	.058

Table A5. Concluded

(b) Concluded

q, lb/ft^2	AOS frequency, Hz	1/2p-p flow angle, deg, for— Vane 1	Vane 2	Vane 3	Wave parameter	Normalized flow angle, deg, for— Vane 1	Vane 2	Vane 3
30	4	0.202	0.230	0.389	0.255	0.034	0.039	0.066
30	4	.220	.189	.311	.256	.037	.032	.052
30	5	.256	.229	.287	.320	.043	.039	.048
30	5	.223	.242	.334	.320	.038	.041	.056
30	10	.204	.248	.278	.638	.034	.042	.047
30	10	.170	.257	.216	.641	.029	.043	.036
40	0	.160	.167	.273	.000	.027	.028	.046
40	0	.274	.285	.257	.000	.046	.048	.043
40	0	.256	.263	.281	.000	.043	.044	.047
40	0	.217	.155	.206	.000	.037	.026	.035
40	1	.248	.253	.527	.055	.042	.043	.089
40	1	.263	.183	.565	.055	.044	.031	.095
40	1	.230	.185	.636	.055	.039	.031	.107
40	1	.192	.319	.677	.055	.032	.054	.114
40	2	.191	.305	.560	.110	.032	.051	.094
40	2	.240	.237	.493	.110	.040	.040	.083
40	2	.257	.211	.528	.110	.043	.036	.089
40	2	.225	.222	.449	.110	.038	.038	.076
40	3	.128	.271	.487	.165	.022	.046	.082
40	3	.222	.298	.469	.165	.037	.050	.079
40	3	.221	.220	.456	.165	.037	.037	.077
40	3	.203	.235	.450	.165	.034	.040	.076
40	4	.230	.261	.394	.220	.039	.044	.066
40	4	.227	.224	.393	.220	.038	.038	.066
40	4	.211	.215	.377	.219	.036	.036	.064
40	4	.225	.252	.398	.220	.038	.043	.067
40	5	.263	.222	.276	.274	.044	.037	.047
40	5	.200	.260	.309	.275	.034	.044	.052
40	5	.218	.228	.265	.274	.037	.039	.045
40	5	.212	.294	.306	.274	.036	.050	.052
40	10	.216	.189	.300	.550	.036	.032	.051
40	10	.107	.217	.266	.550	.018	.037	.045
40	10	.269	.204	.262	.550	.045	.034	.044
40	10	.257	.257	.300	.550	.043	.043	.051
50	0	.283	.071	.254	.000	.048	.012	.043
50	0	.253	.068	.259	.000	.043	.011	.044
50	1	.239	.110	.594	.049	.040	.019	.100
50	1	.240	.117	.616	.049	.040	.020	.104
50	2	.171	.159	.567	.098	.029	.027	.096
50	2	.237	.124	.601	.098	.040	.021	.101
50	3	.195	.119	.533	.148	.033	.020	.090
50	3	.236	.136	.531	.148	.040	.023	.090
50	4	.201	.141	.418	.197	.034	.024	.071
50	4	.250	.109	.450	.196	.042	.018	.076
50	5	.187	.129	.407	.245	.032	.022	.069
50	5	.228	.183	.393	.245	.039	.031	.066
50	10	.183	.190	.288	.491	.031	.032	.049
50	10	.197	.191	.287	.491	.033	.032	.048

Table A6. Flow-Angularity Measurement for Station 67 West

(a) Alpha (vertical) calibration rig position

[There was a problem with alpha vane 3, which caused some readings to be erroneous; these points are marked with an asterisk "*"]

q, lb/ft^2	AOS frequency, Hz	1/2p-p flow angle, deg, for— Vane 1	Vane 2	Vane 3	Wave parameter	Normalized flow angle, deg, for— Vane 1	Vane 2	Vane 3
10	1	0.374	1.187	0.479	0.110	0.063	0.200	0.081
10	2	.143	1.075	.378	.221	.024	.181	.064
10	3	.177	.965	.260	.331	.030	.163	.044
10	4	.133	1.052	.217	.441	.022	.177	.037
10	5	.148	1.228	.360	.551	.025	.207	.061
10	6	.170	1.214	*	.658	.029	.205	*
10	10	.240	.316	.262	1.108	.040	.053	.044
20	1	.491	1.031	.838	.078	.083	.174	.141
20	1	.484	1.102	.837	.078	.082	.186	.141
20	1	.567	.931	.848	.077	.096	.157	.143
20	2	.342	.790	.548	.155	.058	.133	.092
20	2	.275	1.010	.578	.155	.046	.170	.097
20	3	.387	.579	.382	.233	.065	.098	.064
20	3	.394	.608	.318	.234	.066	.103	.054
20	3	.378	.655	.366	.232	.064	.110	.062
20	4	.420	.467	.302	.311	.071	.079	.051
20	4	.404	.743	.296	.309	.068	.125	.050
20	4	.402	.330	.283	.313	.068	.056	.048
20	5	.374	.431	.296	.387	.063	.073	.050
20	5	.392	.411	.344	.387	.066	.069	.058
20	5	.397	.463	.270	.391	.067	.078	.046
20	10	.282	.519	.280	.777	.048	.088	.047
20	10	.326	.350	.299	.784	.055	.059	.050
20	10	.273	.677	.257	.777	.046	.114	.043
30	1	.458	1.417	.882	.064	.077	.239	.149
30	2	.328	1.188	.466	.127	.055	.200	.079
30	3	.375	2.239	.372	.191	.063	.378	.063
30	4	.372	1.748	.276	.254	.063	.295	.047
30	5	.409	2.266	.285	.318	.069	.382	.048
30	10	.317	1.180	.272	.637	.053	.199	.046
40	1	.299	3.211	.867	.055	.050	.541	.146
40	1	.523	2.590	.892	.055	.088	.437	.150
40	2	.245	3.832	*	.109	.041	.646	*
40	2	.311	4.641	.580	.109	.052	.783	.098
40	3	.253	3.149	.442	.164	.043	.531	.075
40	3	.279	3.055	.424	.164	.047	.515	.072
40	4	.339	2.573	.306	.219	.057	.434	.052
40	4	.334	2.217	*	.219	.056	.374	*
40	5	.325	2.078	.279	.274	.055	.350	.047
40	5	.351	1.431	.321	.274	.059	.241	.054
40	10	.340	4.714	.295	.549	.057	.795	.050
40	10	.304	3.274	.283	.549	.051	.552	.048
50	1	.501	1.631	.890	.049	.084	.275	.150
50	2	.391	1.708	.614	.098	.066	.288	.104
50	3	.301	.829	.486	.147	.051	.140	.082
50	4	.336	.802	.369	.196	.057	.135	.062
50	5	.412	1.152	*	.244	.069	.194	*
50	10	.364	1.161	.256	.491	.061	.196	.043

Table A6. Concluded

(b) Beta (lateral) calibration rig position

q, lb/ft^2	AOS frequency, Hz	1/2p-p flow angle, deg, for—			Wave parameter	Normalized flow angle, deg, for—		
		Vane 1	Vane 2	Vane 3		Vane 1	Vane 2	Vane 3
10	1	1.780	0.458	0.218	0.110	0.300	0.077	0.037
10	2	1.784	.228	.181	.221	.301	.038	.031
10	3	1.532	.194	.258	.331	.258	.033	.044
10	4	1.010	.216	.213	.441	.170	.036	.036
10	5	.734	.102	.244	.551	.124	.017	.041
10	6	.565	.169	.196	.658	.095	.029	.033
10	10	.312	.159	.241	1.108	.053	.027	.041
20	1	1.931	.224	.294	.078	.326	.038	.050
20	1	1.947	.209	.198	.078	.328	.035	.033
20	1	1.927	.214	.244	.077	.325	.036	.041
20	2	1.486	.221	.160	.155	.251	.037	.027
20	2	1.626	.230	.220	.155	.274	.039	.037
20	3	1.283	.200	.263	.233	.216	.034	.044
20	3	1.186	.155	.246	.234	.200	.026	.041
20	3	1.401	.258	.265	.232	.236	.043	.045
20	4	1.182	.223	.201	.311	.199	.038	.034
20	4	.935	.203	.226	.309	.158	.034	.038
20	4	.963	.194	.290	.313	.162	.033	.049
20	5	.901	.238	.261	.387	.152	.040	.044
20	5	.794	.195	.213	.387	.134	.033	.036
20	5	.820	.195	.252	.391	.138	.033	.043
20	10	.484	.152	.177	.777	.082	.026	.030
20	10	.407	.209	.200	.784	.069	.035	.034
20	10	.398	.132	.210	.777	.067	.022	.035
30	1	2.046	.234	.250	.064	.345	.039	.042
30	2	1.831	.234	.195	.127	.309	.040	.033
30	3	1.347	.227	.156	.191	.227	.038	.026
30	4	1.455	.225	.154	.254	.245	.038	.026
30	5	.987	.198	.212	.318	.166	.033	.036
30	10	.997	.170	.183	.637	.168	.029	.031
40	1	2.170	.192	.229	.055	.366	.032	.039
40	1	2.077	.229	.222	.055	.350	.039	.037
40	2	1.668	.213	.235	.109	.281	.036	.040
40	2	1.684	.237	.241	.109	.284	.040	.041
40	3	1.094	.219	.227	.164	.184	.037	.038
40	3	1.094	.202	.237	.164	.185	.034	.040
40	4	.951	.205	.201	.219	.160	.034	.034
40	4	.929	.235	.270	.219	.157	.040	.045
40	5	.839	.199	.254	.274	.141	.034	.043
40	5	.827	.174	.186	.274	.139	.029	.031
40	10	.416	.131	.184	.549	.070	.022	.031
40	10	.742	.116	.262	.549	.125	.020	.044
50	1	2.062	.208	.227	.049	.348	.035	.038
50	2	1.510	.185	.272	.098	.255	.031	.046
50	3	1.180	.207	.254	.147	.199	.035	.043
50	4	1.012	.187	.235	.196	.171	.032	.040
50	5	.907	.219	.229	.244	.153	.037	.039
50	10	.414	.163	.231	.491	.070	.027	.039

Table A7. Flow-Angularity Measurement for Station 67 East

(a) Alpha (vertical) calibration rig position

[There was a problem with alpha vane 3, which caused some readings to be erroneous; these points are marked with an asterisk "*"]

q, lb/ft^2	AOS frequency, Hz	1/2p-p flow angle, deg, for—			Wave parameter	Normalized flow angle, deg, for—		
		Vane 1	Vane 2	Vane 3		Vane 1	Vane 2	Vane 3
10	1	0.376	0.879	0.317	0.110	0.063	0.148	0.053
10	2	.314	.366	.277	.220	.053	.062	.047
10	3	.560	.514	.346	.332	.094	.087	.058
10	4	.234	.088	.235	.446	.039	.015	.040
10	5	.043	.189	.197	.552	.007	.032	.033
10	6	.397	.045	.221	.665	.067	.008	.037
10	8	.253	.424	.225	.883	.043	.072	.038
10	10	.256	.207	.190	1.115	.043	.035	.032
20	1	.776	1.010	.274	.078	.131	.170	.046
20	1	.696	.791	.318	.078	.117	.133	.054
20	2	.319	.583	*	.157	.054	.098	*
20	2	.421	.562	.335	.156	.071	.095	.056
20	3	.257	.160	.359	.234	.043	.027	.061
20	3	.454	.283	.365	.235	.077	.048	.062
20	4	.784	.462	.345	.312	.132	.078	.058
20	4	.334	.209	.351	.312	.056	.035	.059
20	5	.644	.385	.362	.389	.109	.065	.061
20	5	.332	.245	.411	.390	.056	.041	.069
20	10	.342	.354	.285	.781	.058	.060	.048
20	10	.407	.313	.294	.779	.069	.053	.050
30	1	.797	1.045	.310	.064	.134	.176	.052
30	2	.409	.675	.223	.127	.069	.114	.038
30	3	.324	.644	.282	.191	.055	.109	.048
30	4	.236	.582	.192	.254	.040	.098	.032
30	5	.223	.639	.264	.319	.038	.108	.045
30	10	.228	.669	.203	.637	.038	.113	.034
40	1	.818	.988	.285	.055	.138	.167	.048
40	1	.698	1.097	.259	.055	.118	.185	.044
40	2	.479	.796	.223	.110	.081	.134	.038
40	2	.578	.778	.169	.110	.097	.131	.028
40	3	.362	.492	.212	.165	.061	.083	.036
40	3	.358	.479	.231	.165	.060	.081	.039
40	4	.285	.466	.266	.219	.048	.079	.045
40	4	.294	.675	.260	.219	.050	.114	.044
40	5	.247	.688	.206	.274	.042	.116	.035
40	5	.246	.415	.232	.275	.041	.070	.039
40	10	.218	.319	.215	.550	.037	.054	.036
40	10	.203	.457	.227	.550	.034	.077	.038
50	1	.835	1.095	.312	.049	.141	.185	.053
50	2	.708	1.004	.230	.098	.119	.169	.039
50	3	.431	.719	.230	.147	.073	.121	.039
50	4	.317	.389	.219	.196	.053	.066	.037
50	5	.172	.686	.294	.245	.029	.116	.050
50	6	.256	.555	.236	.294	.043	.094	.040
50	8	.222	.773	.252	.392	.037	.130	.042
50	10	.242	.515	.238	.491	.041	.087	.040

Table A7. Concluded

(b) Beta (lateral) calibration rig position

q, lb/ft^2	AOS frequency, Hz	1/2p-p flow angle, deg, for— Vane 1	Vane 2	Vane 3	Wave parameter	Normalized flow angle, deg, for— Vane 1	Vane 2	Vane 3
10	1	0.625	0.102	0.382	0.110	0.105	0.017	0.064
10	2	.593	.083	.376	.220	.100	.014	.063
10	3	.583	.081	.308	.332	.098	.014	.052
10	4	.548	.079	.327	.446	.092	.013	.055
10	5	.509	.175	.289	.552	.086	.030	.049
10	6	.488	.007	.288	.665	.082	.001	.049
10	8	.586	.043	.243	.883	.099	.007	.041
10	10	.528	.074	.246	1.115	.089	.013	.042
20	1	.283	.138	.517	.078	.048	.023	.087
20	1	.504	.185	.584	.078	.085	.031	.098
20	2	.259	.158	.363	.157	.044	.027	.061
20	2	.488	.126	.399	.156	.082	.021	.067
20	3	.500	.181	.288	.234	.084	.031	.049
20	3	.390	.154	.272	.235	.066	.026	.046
20	4	.374	.121	.328	.312	.063	.020	.055
20	4	.438	.165	.339	.312	.074	.028	.057
20	5	.450	.176	.295	.389	.076	.030	.050
20	5	.395	.186	.316	.390	.067	.031	.053
20	10	.487	.201	.268	.781	.082	.034	.045
20	10	.409	.198	.258	.779	.069	.033	.044
30	1	.489	.158	.639	.064	.082	.027	.108
30	2	.516	.128	.557	.127	.087	.022	.094
30	3	.439	.084	.371	.191	.074	.014	.063
30	4	.400	.168	.313	.254	.067	.028	.053
30	5	.394	.153	.346	.319	.066	.026	.058
30	10	.362	.194	.260	.637	.061	.033	.044
40	1	.638	.166	.639	.055	.108	.028	.108
40	1	.301	.194	.552	.055	.051	.033	.093
40	2	.463	.176	.549	.110	.078	.030	.093
40	2	.366	.188	.490	.110	.062	.032	.083
40	3	.369	.147	.403	.165	.062	.025	.068
40	3	.631	.183	.399	.165	.106	.031	.067
40	4	.439	.199	.312	.219	.074	.033	.053
40	4	.377	.148	.343	.219	.064	.025	.058
40	5	.357	.185	.384	.274	.060	.031	.065
40	5	.416	.181	.353	.275	.070	.031	.060
40	10	.392	.199	.315	.550	.066	.034	.053
40	10	.439	.189	.296	.550	.074	.032	.050
50	1	.633	.123	.597	.049	.107	.021	.101
50	2	.421	.110	.498	.098	.071	.019	.084
50	3	.707	.021	.433	.147	.119	.004	.073
50	4	.285	.072	.405	.196	.048	.012	.068
50	5	.516	.082	.356	.245	.087	.014	.060
50	6	.611	.065	.347	.294	.103	.011	.059
50	8	.781	.072	.326	.392	.132	.012	.055
50	10	.692	.108	.283	.491	.117	.018	.048

References

1. Drees, Jan M.; and Harvey, Keith W.: Helicopter Gust Response at High Forward Speed. AIAA Paper No. 68-981, Oct. 1968.
2. Arcidiacono, Peter J.; Bergquist, Russell R.; and Alexander, W. T., Jr.: Helicopter Gust Response Characteristics Including Unsteady Aerodynamic Stall Effects. *Rotorcraft Dynamics*, NASA SP-352, 1974, pp. 91–100.
3. Jenkins, Julian L., Jr.; and Yeager, William T., Jr.: *An Analysis of the Gust-Induced Overspeed Trends of Helicopter Rotors.* NASA TP-1213, AVRADCOM TR-78-24, 1978.
4. Bir, Gunjit Singh; and Chopra, Inderjit: Gust Response of Hingeless Rotors. *J. American Helicopter Soc.*, vol. 31, no. 2, Apr. 1986, pp. 33–46.
5. Abbott, Frank T., Jr.: Brief Description of the Characteristics of the Langley Transonic Dynamics Tunnel Airstream Oscillator. *Meeting on Aircraft Response to Turbulence*, NASA TM-82340, 1968, pp. 6.1–6.11.
6. Gilman, Jean, Jr.; and Bennett, Robert M.: A Wind-Tunnel Technique for Measuring Frequency-Response Functions for Gust Load Analyses. AIAA Paper No. 65-787, Nov. 1965.
7. Redd, L. Tracy; Hanson, Perry W.; and Wynne, Eleanor C.: *Evaluation of a Wind-Tunnel Gust Response Technique Including Correlations With Analytical and Flight Test Results.* NASA TP-1501, 1979.
8. Lee, Charles: Weight Considerations in Dynamically Similar Model Rotor Design. SAWE Paper No. 659, May 1968.
9. Mantay, Wayne R.; Yeager, William T., Jr.; Hamouda, M-Nabil; Cramer, Robert G., Jr.; and Langston, Chester W.: *Aeroelastic Model Helicopter Rotor Testing in the Langley TDT.* NASA TM-86440, USAAVSCOM TM 85-B-5, 1985.
10. Kvaternik, Raymond George: Studies in Tilt-Rotor VTOL Aircraft Aeroelasticity. Ph.D. Thesis, Case Western Reserve Univ., 1973.

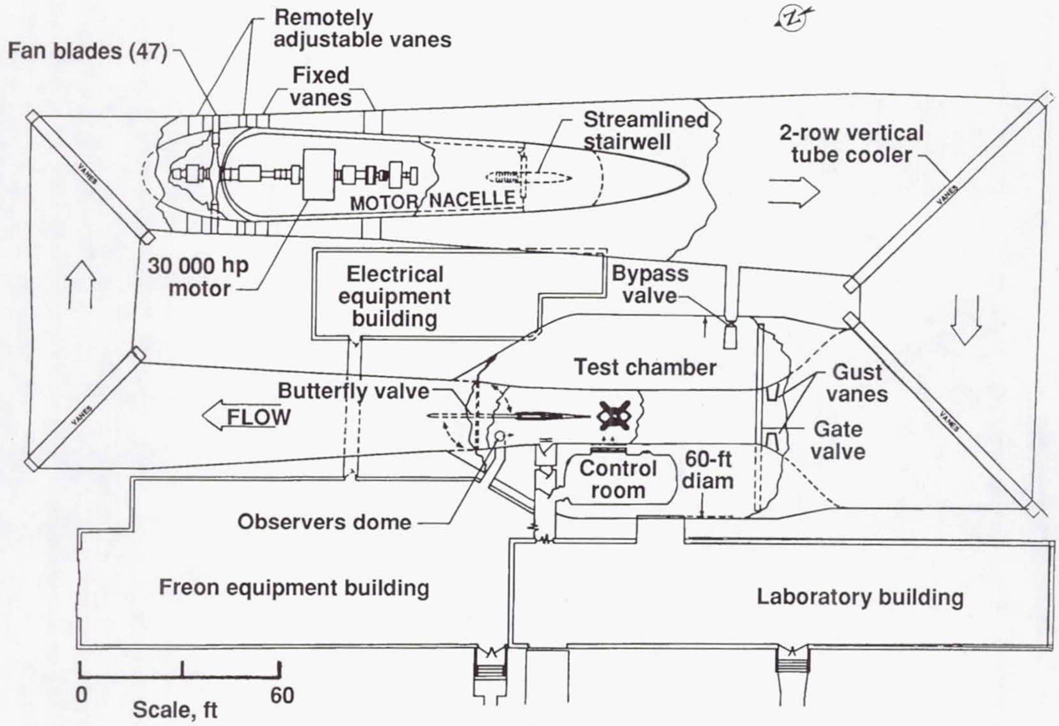

Figure 1. General arrangement of Langley Transonic Dynamics Tunnel.

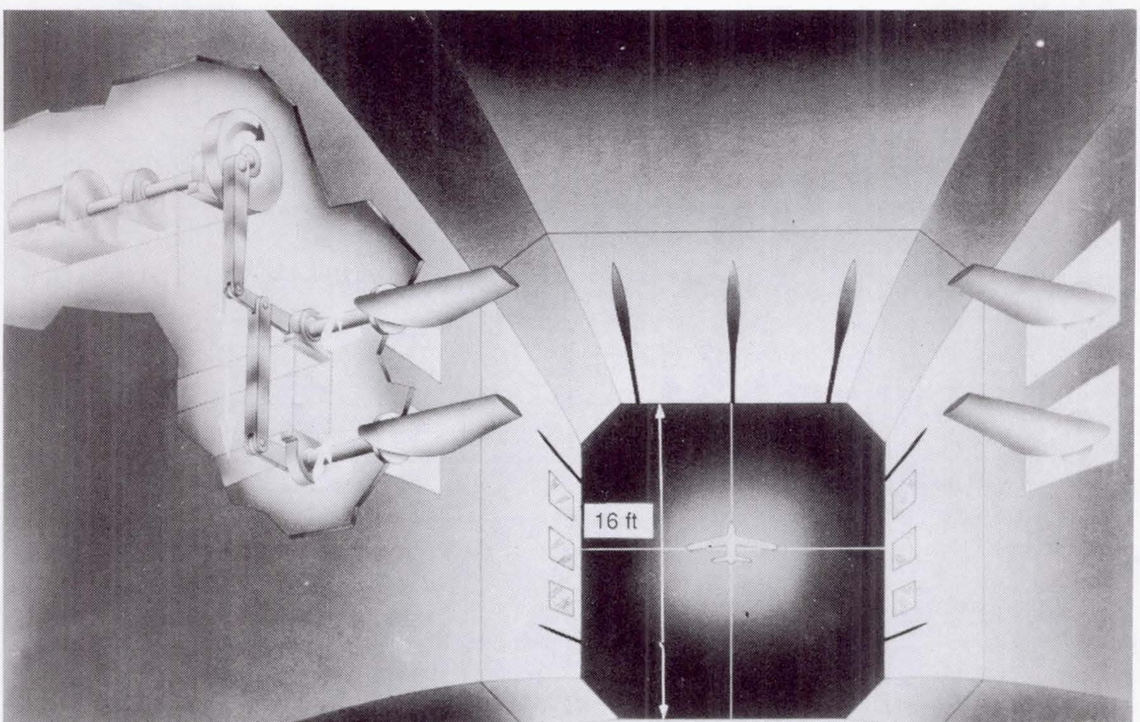

L-71-301

Figure 2. Sketch of airstream oscillator vanes with cutaway schematic of mechanism.

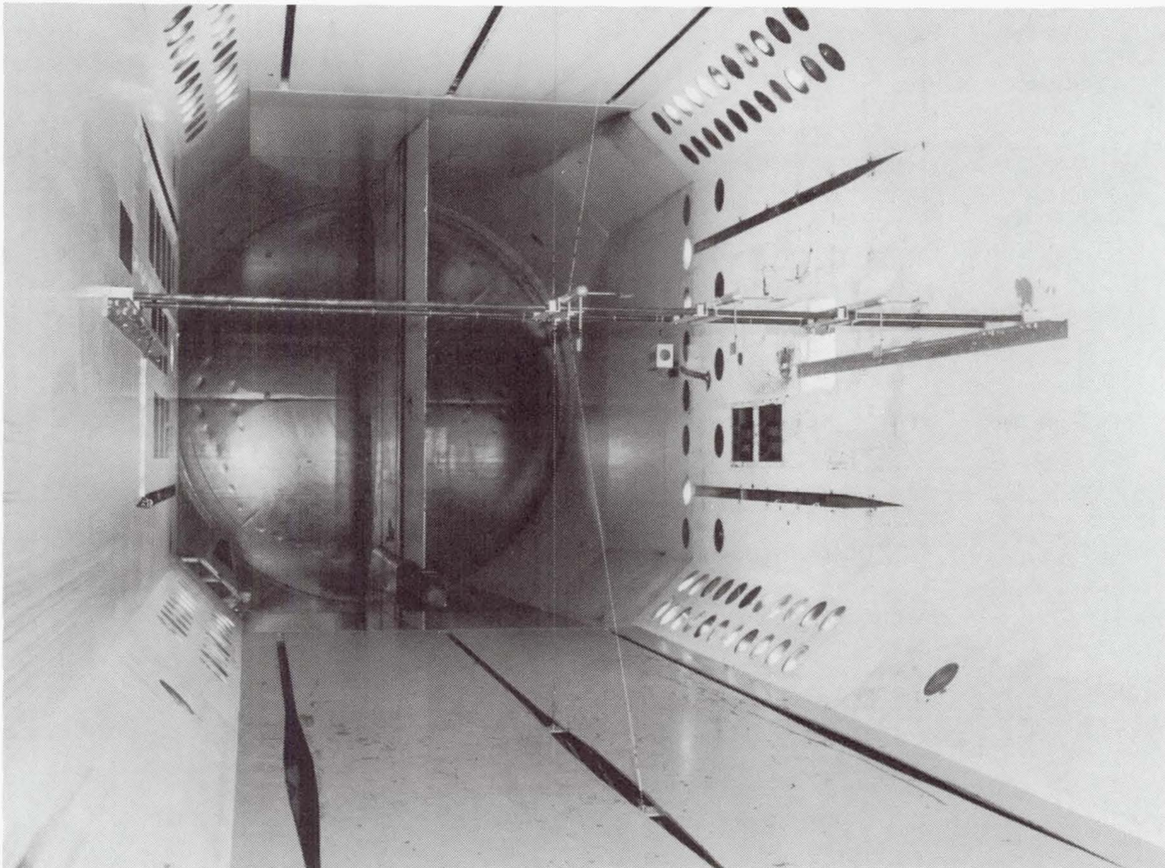

Figure 3. Airstream calibration rig mounted in Langley Transonic Dynamics Tunnel.

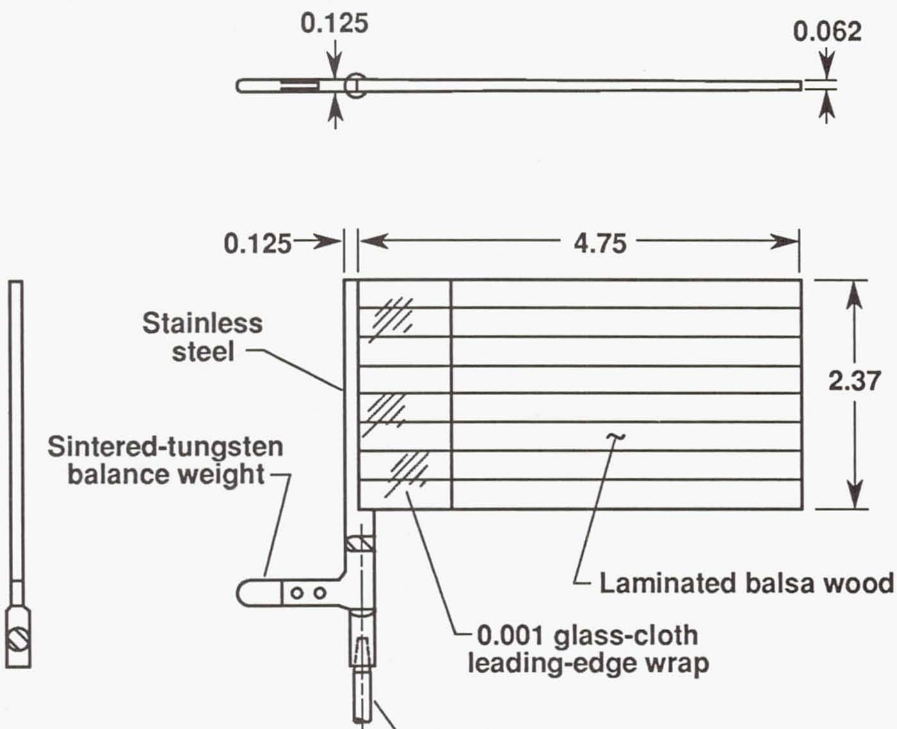

Figure 4. Flow-direction vane. (Dimensions are in inches.)

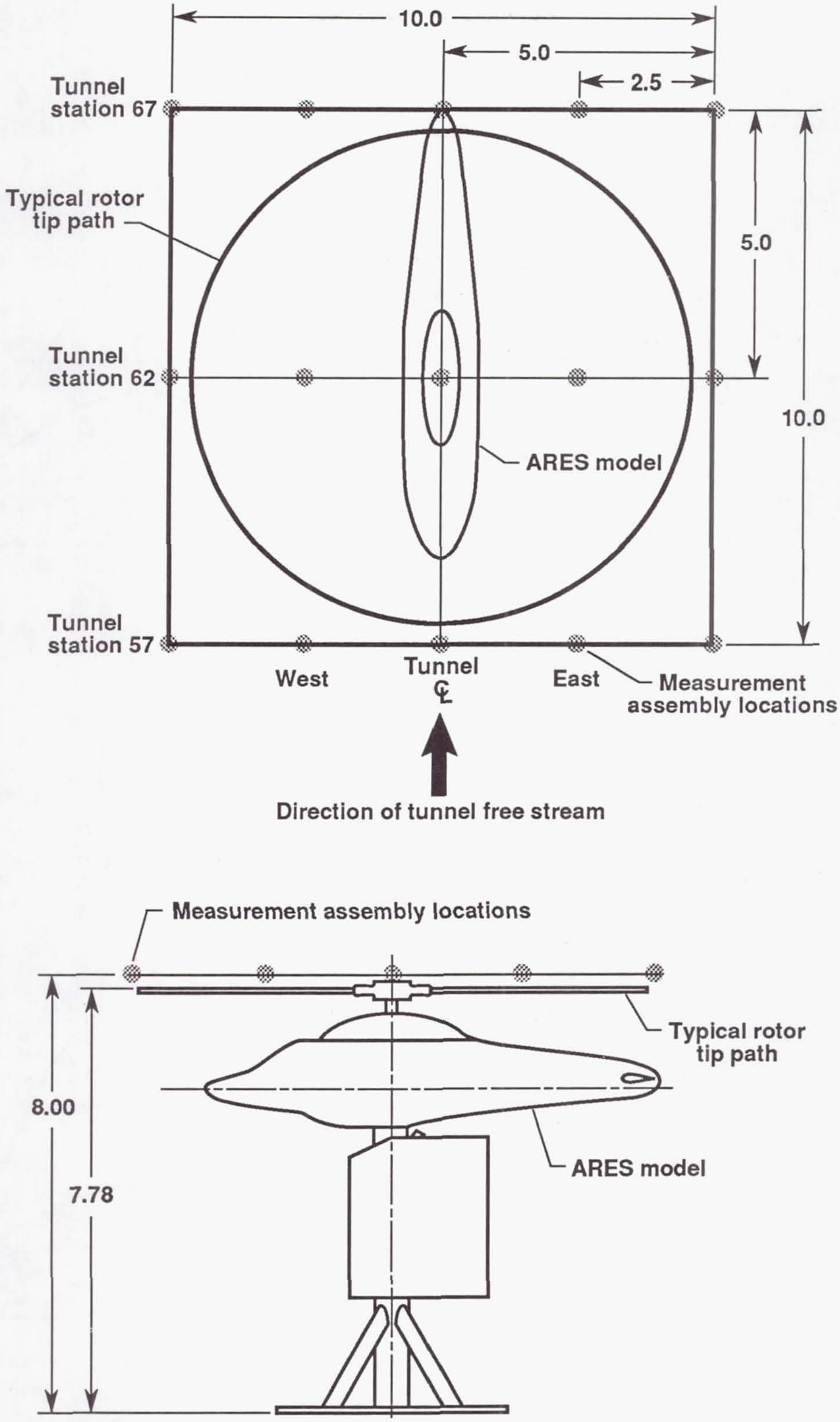

Figure 5. Flow-measurement assembly locations. (Dimensions are in feet.)

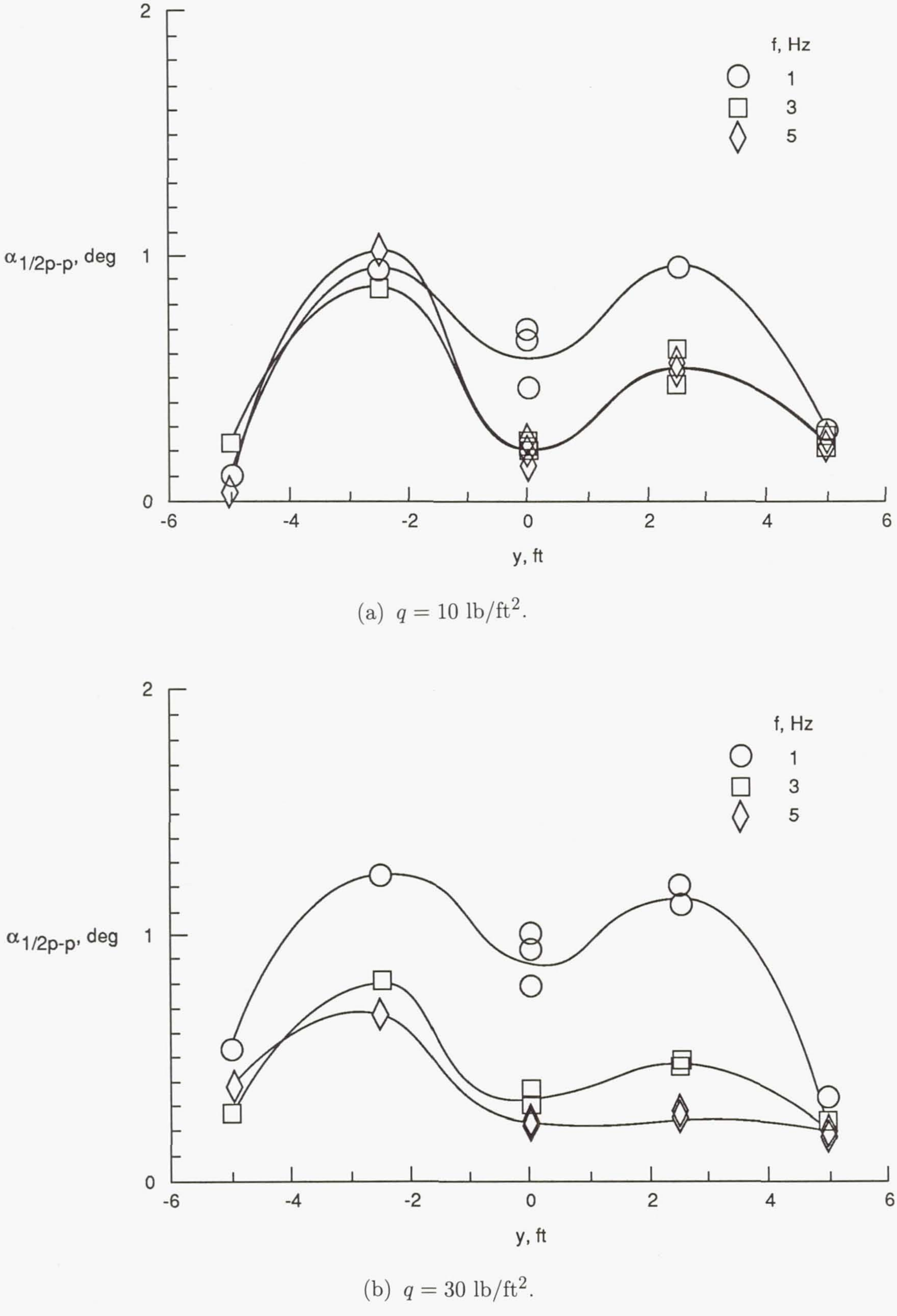

(a) $q = 10$ lb/ft^2.

(b) $q = 30$ lb/ft^2.

Figure 6. Spanwise variation of vertical-flow angle at tunnel station 62.

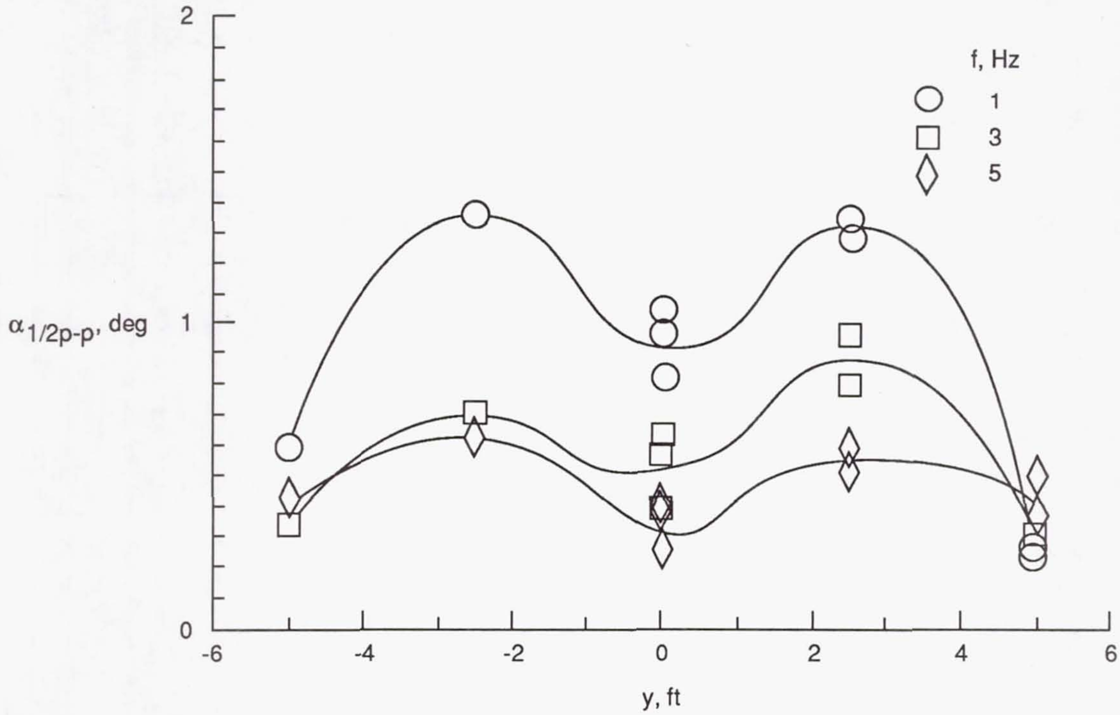

(c) $q = 50\ \text{lb/ft}^2$.

Figure 6. Concluded.

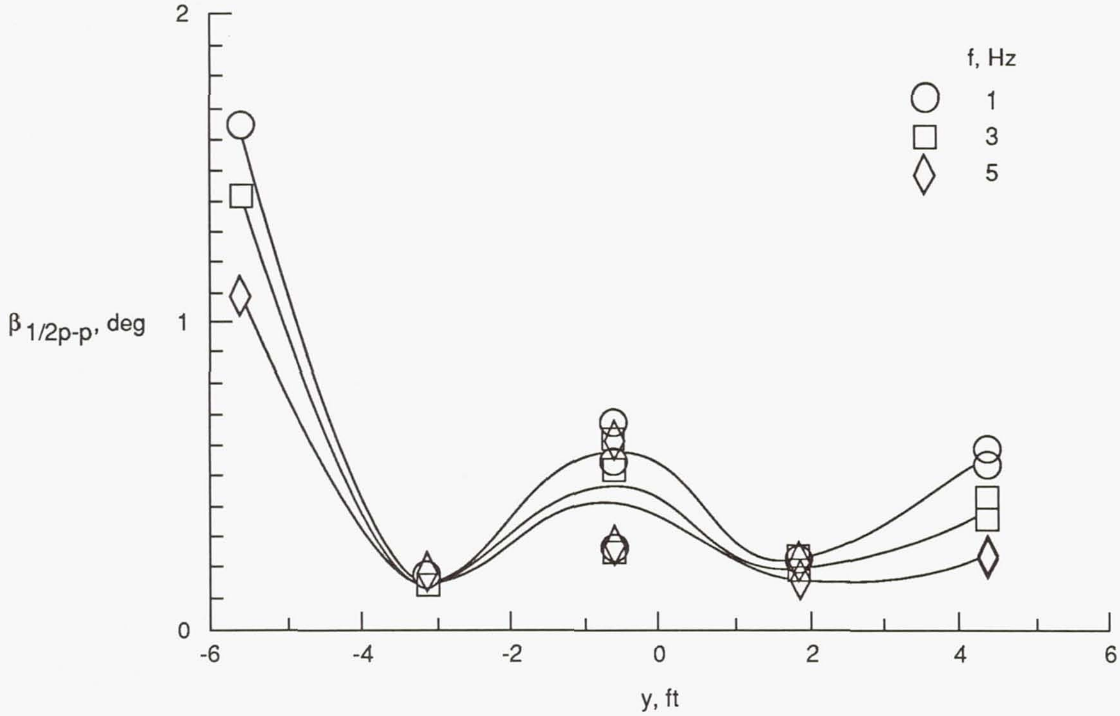

(a) $q = 10$ lb/ft^2.

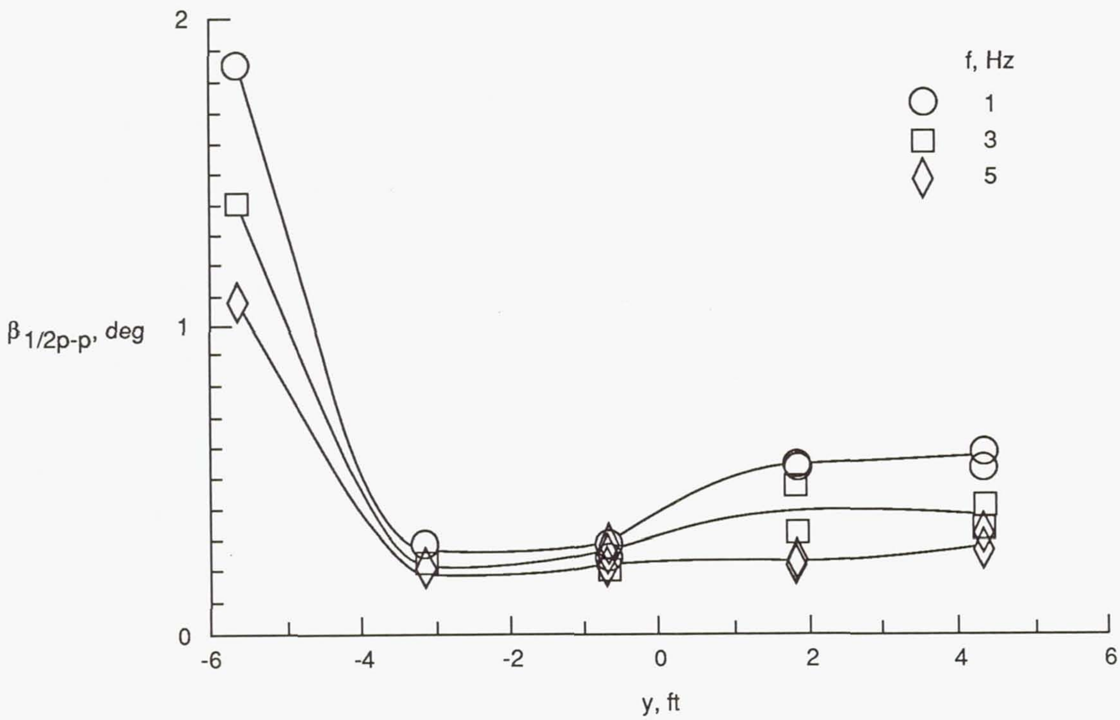

(b) $q = 30$ lb/ft^2.

Figure 7. Spanwise variation of lateral-flow angle at tunnel station 62.

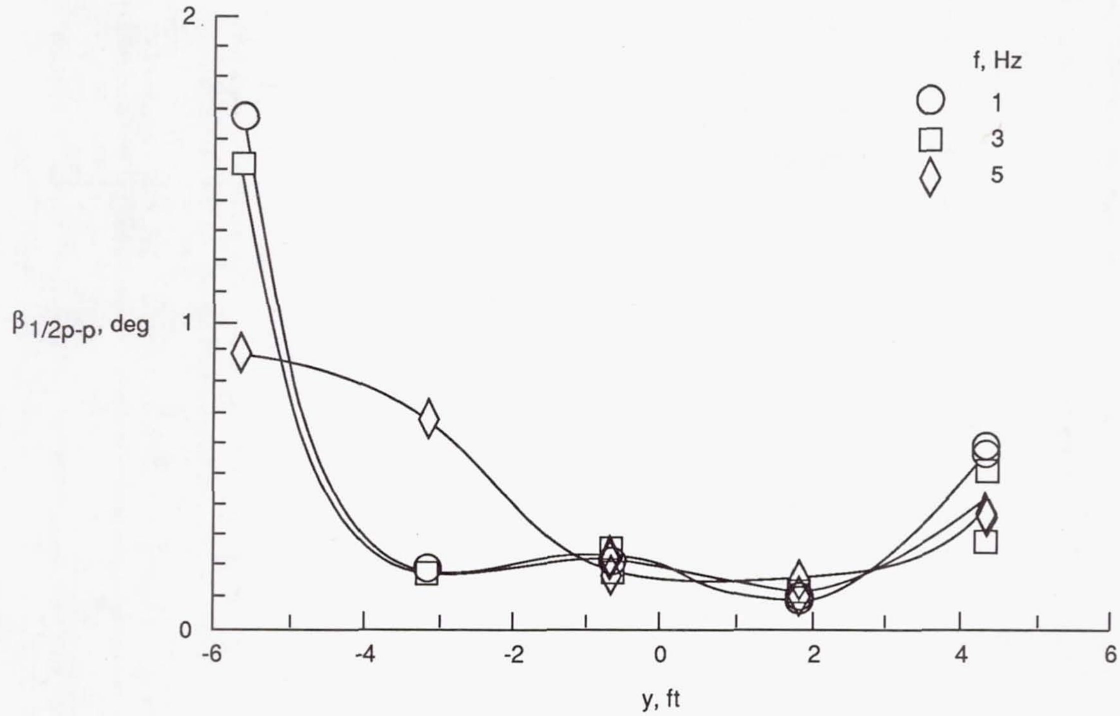

(c) $q = 50$ lb/ft^2.

Figure 7. Concluded.

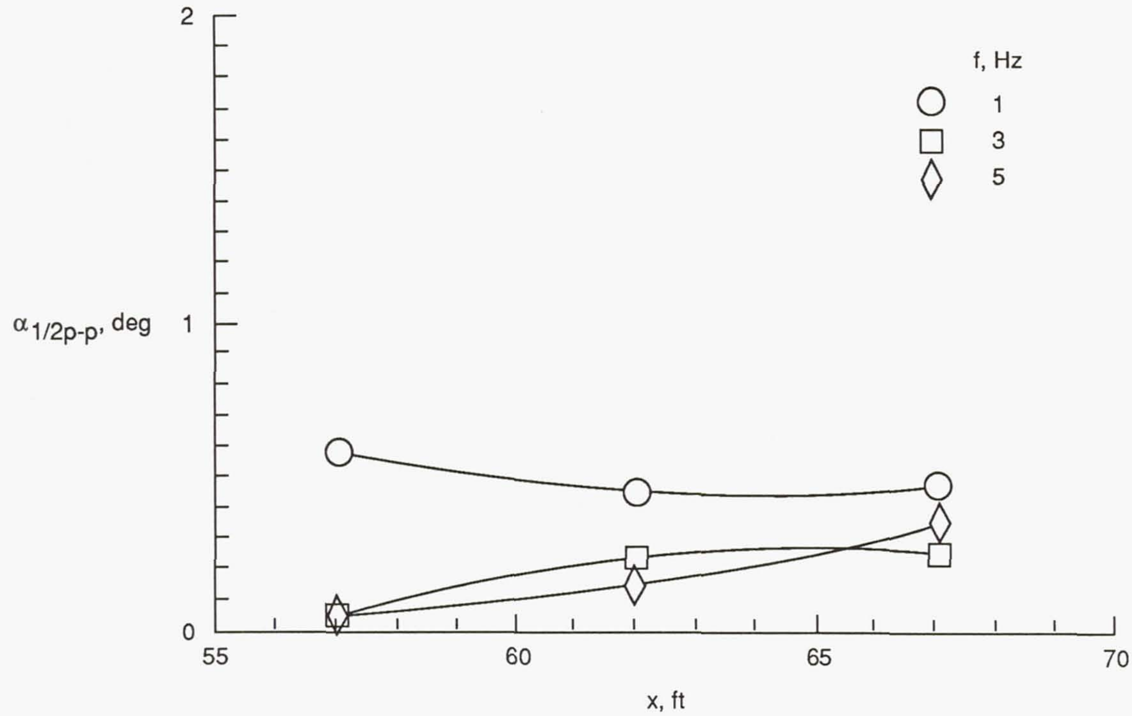

(a) $q = 10$ lb/ft^2.

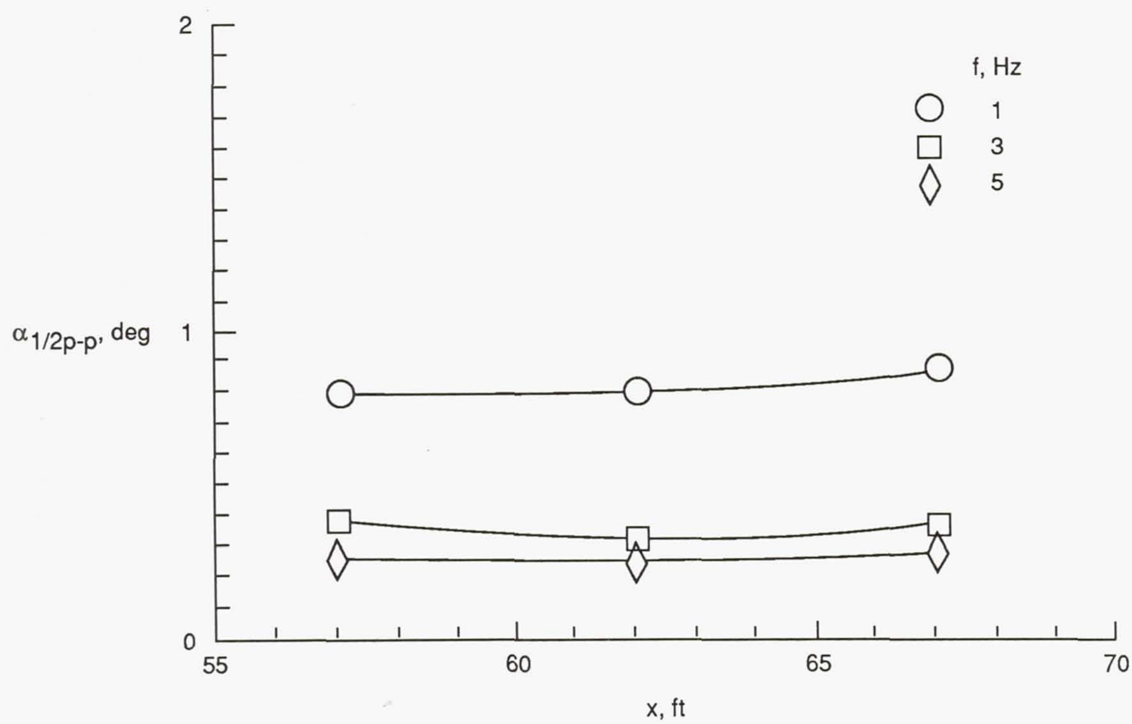

(b) $q = 30$ lb/ft^2.

Figure 8. Longitudinal variation of vertical-flow angle at tunnel centerline.

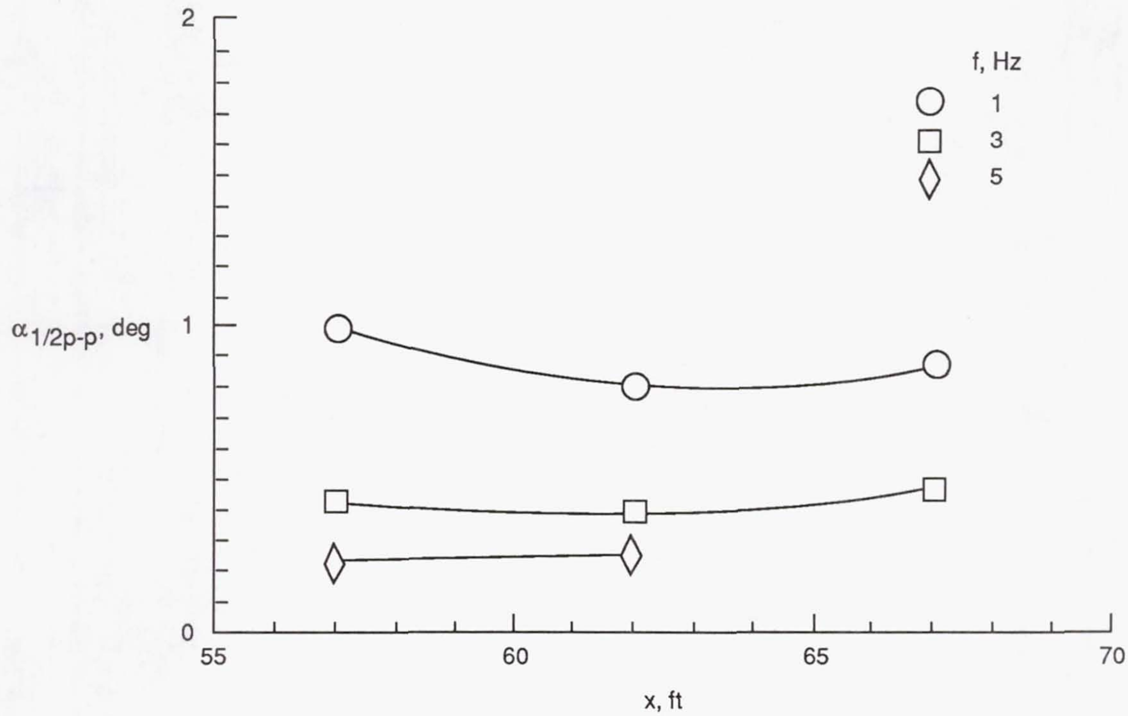

(c) $q = 50$ lb/ft^2.

Figure 8. Concluded.

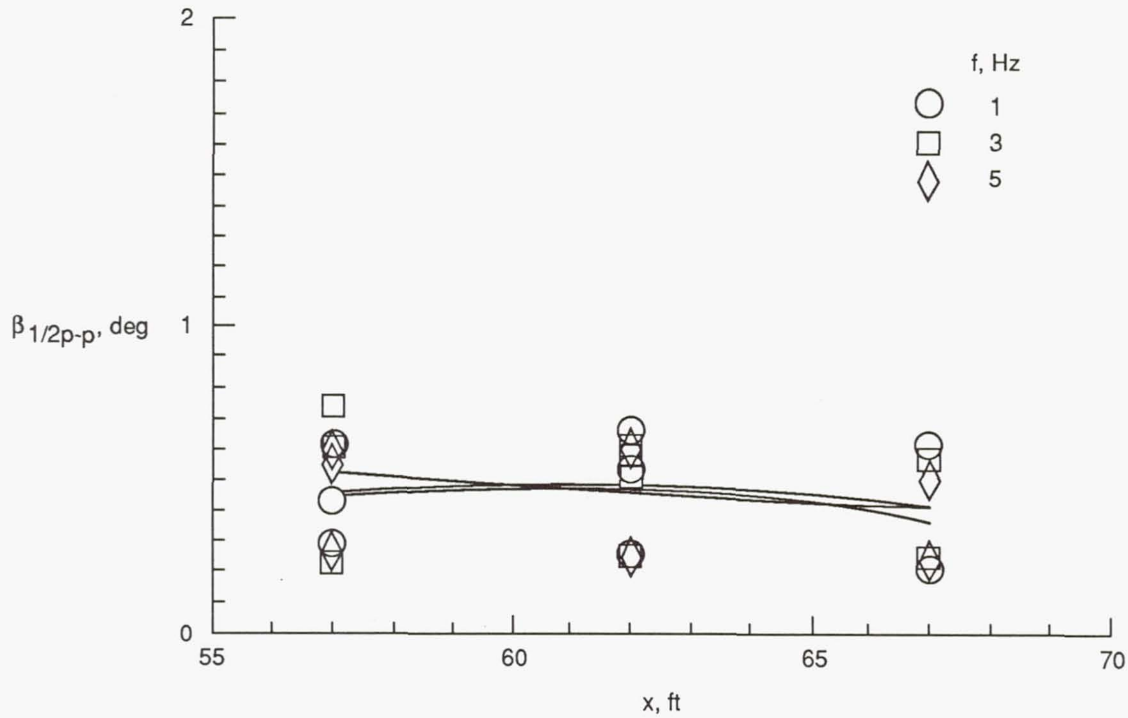

(a) $q = 10$ lb/ft^2.

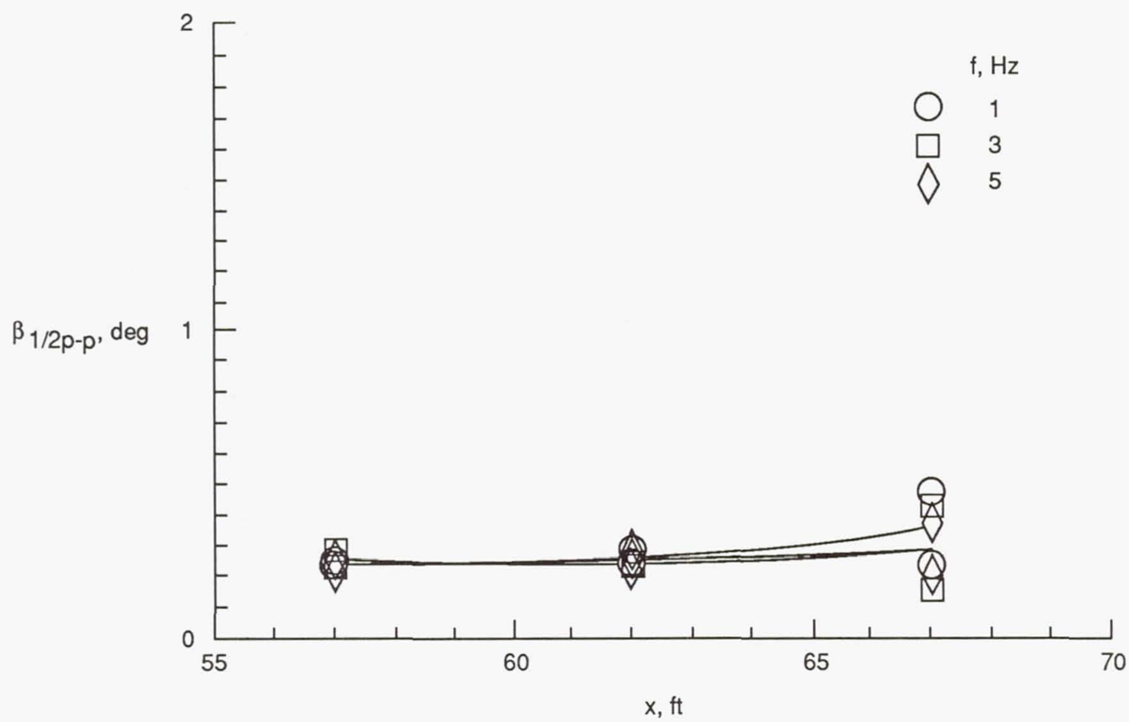

(b) $q = 30$ lb/ft^2.

Figure 9. Longitudinal variation of lateral-flow angle 8 in. from tunnel centerline.

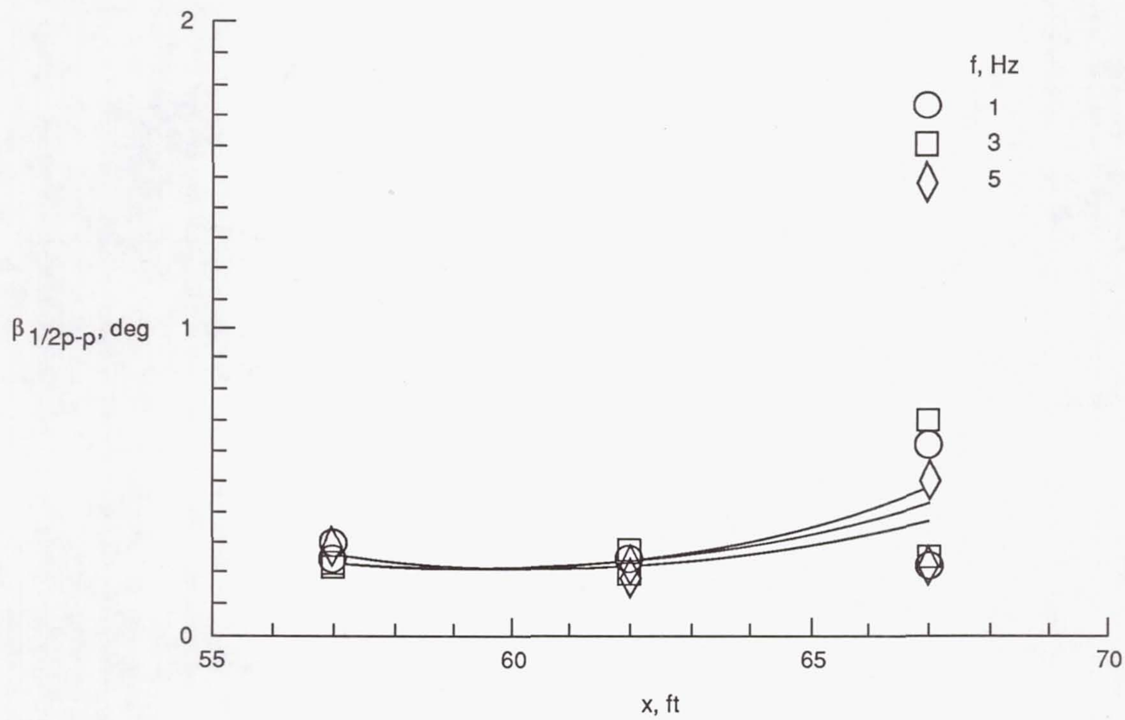

(c) $q = 50$ lb/ft^2.

Figure 9. Concluded.

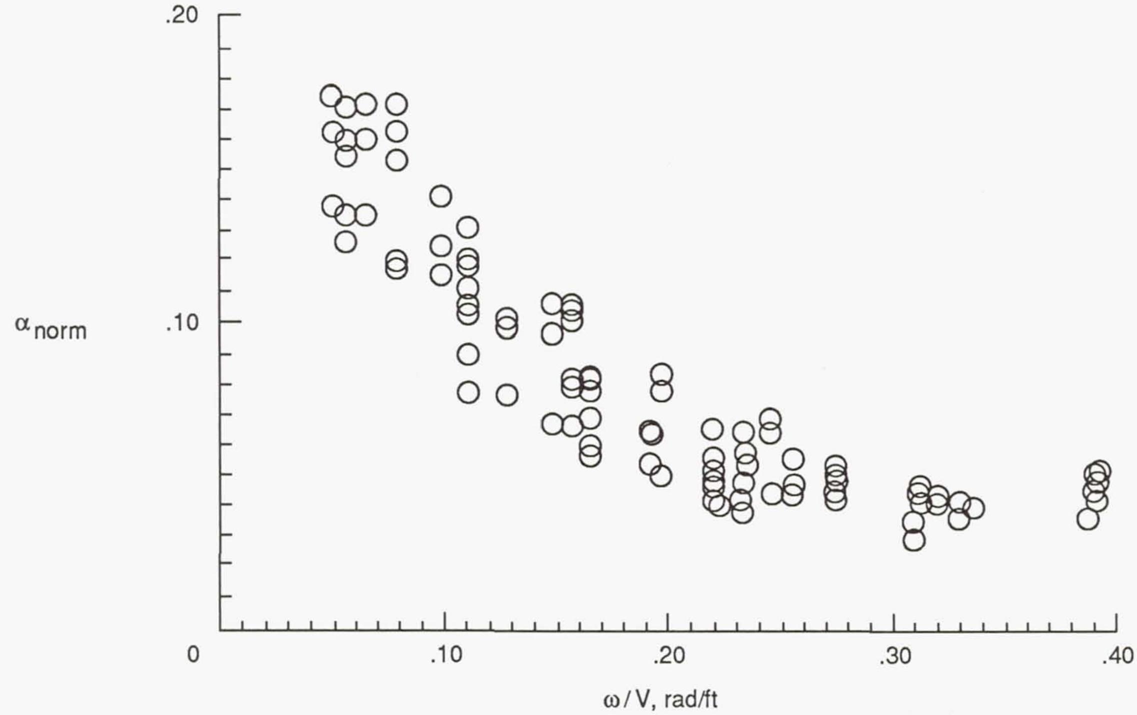

Figure 10. Variation of normalized vertical-flow angle with wave parameter at tunnel centerline and station 62.

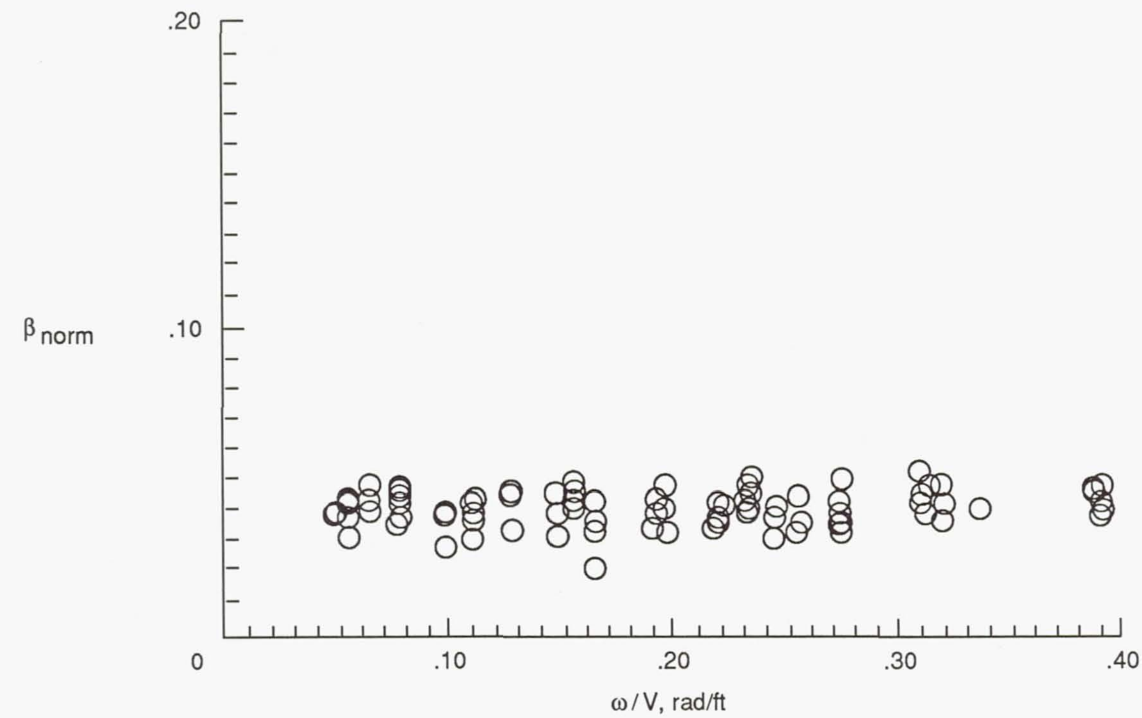

Figure 11. Variation of normalized lateral-flow angle with wave parameter at tunnel centerline and station 62.

NASA
National Aeronautics and Space Administration

Report Documentation Page

1. Report No.	2. Government Accession No.	3. Recipient's Catalog No.
NASA TM-4224 AVSCOM TR-90-B-007		

4. Title and Subtitle
Wind-Tunnel Survey of an Oscillating Flow Field for Application to Model Helicopter Rotor Testing

5. Report Date
December 1990

6. Performing Organization Code

7. Author(s)
Paul H. Mirick, M-Nabil H. Hamouda, and William T. Yeager, Jr.

8. Performing Organization Report No.
L-16757

9. Performing Organization Name and Address
Aerostructures Directorate
USAARTA-AVSCOM
Langley Research Center
Hampton, VA 23665-5225

10. Work Unit No.
505-63-51-03

11. Contract or Grant No.

12. Sponsoring Agency Name and Address
National Aeronautics and Space Administration
Washington, DC 20546-0001
and
U.S. Army Aviation Systems Command
St. Louis, MO 63120-1798

13. Type of Report and Period Covered
Technical Memorandum

14. Army Project No.
1L162211A47AB

15. Supplementary Notes
Paul H. Mirick and William T. Yeager, Jr.: Aerostructures Directorate, USAARTA-AVSCOM.
M-Nabil H. Hamouda: Lockheed Engineering & Sciences Company, Hampton, Virginia.

16. Abstract
A survey was conducted of the flow field produced by the airstream oscillator system (AOS) in the Langley Transonic Dynamics Tunnel (TDT). The magnitude of a simulated gust field was measured at 15 locations in the plane of a typical model helicopter rotor when tested in the TDT using the aeroelastic rotor experimental system (ARES) model. These measurements were made over a range of tunnel dynamic pressures typical of those used for an ARES test. The data indicate that the gust field produced by the AOS is nonuniform across the tunnel test section, but that it should be sufficient to excite a model rotor.

17. Key Words (Suggested by Authors(s))
Helicopter
Gust
Wind-tunnel techniques

18. Distribution Statement
Unclassified—Unlimited

Subject Category 09

19. Security Classif. (of this report)	20. Security Classif. (of this page)	21. No. of Pages	22. Price
Unclassified	Unclassified	35	A03

NASA FORM 1626 OCT 86

NASA-Langley, 1990

For sale by the National Technical Information Service, Springfield, Virginia 22161-2171